博士論文

SIRT1 maintains podocyte homeostasis via regulation of actin fiber formation

(SIRT1 はアクチン線維形成の制御を介して糸球体足細胞の恒常性を維持する)

本西 秀太

Table of contents

Abstract

Recent studies highlighted the renoprotective effect of SIRT1, a deacetylase that contributes to cellular regulation. However, its pathophysiological role in podocytes is unclear. I thus investigated the function of SIRT1 in podocytes.

I made podocyte specific *Sirt1* knockout (SIRT1$^{pod-/-}$) mice by crossing *Sirt1*$^{flox/flox}$ mice with podocin-Cre mice. Then, I induced glomerular damage by injection of sheep anti-glomerular basement membrane (GBM) antibody in SIRT1$^{pod-/-}$ or wild-type mice. Seven days after the disease induction, both urinary albumin per creatinine ratio and BUN in SIRT1$^{pod-/-}$ mice were significantly higher than those in wild-type mice and histological injury of glomeruli was also significantly increased in SIRT1$^{pod-/-}$ mice. In western blot analysis of isolated glomeruli, podocyte specific molecules were significantly reduced in SIRT1$^{pod-/-}$ mice, and these findings were confirmed by immunofluorescence study. By electron microscopy, I found that foot process effacement and actin cytoskeleton derangement caused by glomerular disease induction were markedly exacerbated in SIRT1$^{pod-/-}$ mice compared with wild-type mice. Similarly, in *in vitro* study, mild actin cytoskeleton derangement in H$_2$O$_2$-treated podocytes became prominent when the cells were pretreated with SIRT1 inhibitors, while an SIRT1 activator ameliorated the actin cytoskeleton derangement. Cellular motility was also reduced by pharmacological SIRT1 inhibition. Moreover, I assessed actin fiber-binding protein cortactin, and found that SIRT1 deacetylated acetylated cortactin in nucleus and the deacetylated cortac-

tin was transported to cytoplasm for maintenance of actin fiber. Taken together, SIRT1 maintains

podocyte homeostasis and prevents glomerular injury by deacetylating cortactin and the subsequent

maintenance of actin fiber integrity.

Introduction

In kidney, a tubular structure called the nephron filters blood to form urine. A glomerulus is the beginning of the nephron, which is a network of capillaries that performs the first step of filtering blood. The filtration barrier of the glomerulus consists of a fenestrated capillary epithelium, glomerular basement membrane (GBM) and the final barrier formed by podocyte. Podocytes, which are characterized as visceral glomerular epithelial cells, are highly differentiated cells which play an essential role in maintenance of the glomerular tuft and filtration barrier. Foot processes (FPs) of adjacent podocytes regularly interdigitate to form narrow filtration slits that are bridged by the slit diaphragm (SD), a zipper-like structured modified adherens junction [1] (Figure 1S). Podocyte injury is a common feature in glomerular diseases [1-6]. Among several pathophysiological mechanisms of podocyte injury, derangement of actin cytoskeleton is a critical pathological manifestation, because the actin cytoskeleton plays an essential role in maintaining the podocyte structure, including FPs. Actin fibers in podocytes function not only in the maintenance of cellular structure, but also in interactions with various molecules, including structural molecules in the SD [1], [7], [8] (Figure 2S). These findings strongly suggest that the maintenance of actin cytoskeleton is essential to glomerular function and podocyte homeostasis.

SIRT1 (Sirtuin1, silent mating type information regulation 2 [Sir2] homolog) is a NAD$^+$-dependent deacetylase (Figure 3S) that regulates a variety of physiological phenomena such

5

as metabolism, stress response, DNA repair, inflammation, and longevity [9–15]. Most of the effects of SIRT1 depend on its deacetylation activity [9], [10] (Figure 4S). Recent studies have shown that SIRT1 is associated with a number of pathological conditions, including metabolic disorders, cardiovascular diseases, neurodegenerative diseases and cancer in various organs [16–21] (Figure 5S). With regard to the kidney, SIRT1 is reported to have renoprotective functions [22], [23]. As examples, SIRT1 regulates glucose or lipid metabolism, blood pressure, and oxidative stress, which are all closely associated with kidney disease [24–28]. In addition, SIRT1 protects the proximal tubular [29–31], medullary [32], and mesangial cells [33], [34] (Figure 6S). However, the pathophysiological role of SIRT1 expressed in podocytes is unclear, and no report has described the establishment or use of podocyte-specific *Sirt1* knockout mice. Although several studies have suggested the possibility of a protective effect of SIRT1 on podocytes [35], [36], the molecular mechanism of the function of SIRT1 expressed in podocytes remains unclear.

Here, I hypothesized that the protective effect of SIRT1 on podocytes results from its maintenance of actin cytoskeleton, which is a critical factor for podocyte homeostasis. To address this question, I established for the first time podocyte-specific *Sirt1* knockout (SIRT1[pod-/-]) mice and investigated the effect of SIRT1 deletion in podocytes.

Materials and Methods

Reagents and antibodies

Three SIRT1 inhibitors were used: EX-527 (Tocris Bioscience, Bristol, UK), cambinol (Santa Cruz Biotechnology, Santa Cruz, CA, USA), and nicotinamide (Sigma-Aldrich, St. Louis, MO, USA). SIRT1 activator resveratrol was purchased from Tokyo Chemical Industry (Tokyo, Japan). Hydrogen peroxide (H_2O_2) was purchased from Wako Pure Chemical Industries (Tokyo, Japan) and used as a cellular damage inducer *in vitro*.

Sheep anti-glomerular basement membrane (GBM) antibody was kindly provided by Dr. Reiko Inagi in my institute and the obtained antiserum was used as anti-GBM antibody. Polyclonal rabbit anti-SIRT1 (1:300; 07-131) antibody, monoclonal mouse anti-cortactin antibody (1:300; 05-180; clone 4F11), polyclonal rabbit anti-acetyl cortactin antibody (1:200; 09-881) and polyclonal rabbit anti-acetyl-histone H3 antibody (1:5000; 06-599) were purchased from Millipore (Billerica, MA, USA) and used for western blot analysis, immunoprecipitation or immunostaining. Polyclonal rabbit anti-WT-1 antibody (1:200; sc-192), polyclonal rabbit anti-synaptopodin antibody (1:200; sc-50459), polyclonal goat anti-nephrin antibody (1:100; sc-19000) and monoclonal mouse anti-histone H1 antibody (1:100; sc-8030) were obtained from Santa Cruz Biotechnology and used for western blot analysis or immunofluorescence. Polyclonal rabbit anti-actin antibody (1:1000; A2066), polyclonal

rabbit anti-nitrotyrosine antibody (1:300; N0409), Texas Red-conjugated polyclonal rabbit anti-sheep antibody (1:20; SAB3700695), and monoclonal mouse anti-α-tubulin antibody (1:1000; T6199, clone DM1A) were purchased from Sigma-Aldrich. As secondary antibody for immunohistochemistry, biotinylated goat anti-rabbit IgG antibody (1:1000; BA-1000) was obtained from Vector Laboratories (Burlingame, CA, USA). Horseradish peroxidase (HRP)-conjugated goat anti-mouse (1:10000; 170-6516; Bio-Rad Laboratories, Hercules, CA, USA), HRP-conjugated goat anti-rabbit IgG (1:10000; 170-6515; Bio-Rad Laboratories) or HRP-conjugated donkey anti-goat IgG (1:500; sc-2020; Santa Cruz Biotechnology) were used as secondary antibodies for western blot analysis. For immunofluorescence study, fluorescein isothiocyanate (FITC)-conjugated polyclonal swine anti-rabbit immunoglobulin antibody (1:20; F0205; Dako, Carpinteria, CA, USA), Texas Red-conjugated goat anti-rabbit IgG (H+L) (1:20; T2767; Invitrogen, Eugene, OR, USA), Alexa Fluor 546-conjugated goat anti-mouse IgG (H+L) (1:200, A11003, Invitrogen) or FITC-conjugated goat anti-mouse IgG (1:200, 1070-02, Southern Biotechnology Associates, Birmingham, AL, USA) was used as secondary antibody. Alexa Fluor 488 phalloidin (1:40) was purchased from Invitrogen and used for detection of actin fiber in vitro. Hoechst 33258 (1:10000, Sigma-Aldrich) was used for the detection of nucleus.

Animal experiments

Podocyte-specific *Sirt1* knockout (SIRT1$^{pod-/-}$) mice were established by crossing podocin-Cre mice [37] on C57BL/6J background with *Sirt1*$^{flox/flox}$ mice on the same background, as described previously (kindly provided by Dr. Kazuyuki Tobe, University of Toyama). To evaluate the basal state of SIRT1$^{pod-/-}$ mice, I measured body-weight, blood pressure, pulse rate, blood urea nitrogen (BUN) and urinary-albumin creatinine ratio (U-alb/cre) in male SIRT1$^{pod-/-}$ mice and wild-type mice at 13-14 weeks of age. For glomerular disease induction, male SIRT1$^{pod-/-}$ and wild-type mice were administered sheep anti-GBM antibody (0.7 ml/kg) at 13-14 weeks of age. Seven days after administration, serum and urine (24-h) were collected to measure BUN and U-alb/cre. The experimental mice were then sacrificed and the kidneys were removed for histological analysis or isolation of glomeruli.

Isolation of glomeruli

Glomeruli were isolated using a previously described method [38], with some modification. Briefly, I placed a catheter into the aorta of the mouse, and perfused magnetic Dynabeads (Invitrogen) through the catheter. After removal, kidneys were minced into small pieces, digested by collagenase and DNase, and filtered. After washing several times, the glomeruli were collected using a magnet. The purity of glomeruli was confirmed to be more than 95% in each sample by phase-contrast microsco-

py.

Histological analysis of glomeruli by PAS staining and immunohistochemistry

Glomerular injury was evaluated by optical microscopy of formalin-fixed sections (3-μm thickness) stained with Periodic acid-Schiff (PAS) reagent. For quantitative comparison, 100 glomeruli were observed and the number of damaged glomeruli, such as those with crescent formation or tuft necrosis, was counted. The ratio of injured glomeruli to all glomeruli was calculated for every group of mice.

In immunohistochemical analysis, kidneys were fixed in formalin solution or methyl Carnoy's solution and embedded in paraffin. Sections of 3-μm thickness were incubated with primary antibody for 12 h at 4 °C, then with biotinylated secondary antibodies for 1 h, and HRP-conjugated avidin D (1:2000; A-2004; Vector Laboratories) for 30 minutes. Color was developed by incubation with diaminobenzidine and hydrogen peroxide (Wako Pure Chemical Industries) at 37 °C.

Immunofluorescence study

Kidneys were removed from mice, embedded in O.C.T. compound (Sakura Finetek Japan, Tokyo, Japan), and frozen on dry ice. The frozen block was cut into 4-μm sections, which were then fixed in

methanol/acetone (1:1) and incubated with primary antibody for 12 h. They were subsequently incubated with fluorescence-conjugated secondary antibody and/or fluorescence-conjugated probes for 1 h in dark conditions.

Electron microscopy

For electron microscopic examination, kidney tissue was fixed in 2.5% glutaraldehyde solution in phosphate buffer (pH 7.4), then postfixed with 1% osmium tetroxide, dehydrated, and embedded in Epok 812. Ultrathin sections were stained with uranyl acetate and lead citrate, and then examined with an electron microscope (model H7100, Hitachi Corp., Tokyo, Japan).

Cell culture

Conditionally immortalized murine podocytes were generated and characterized as described previously [39]. The cells were grown in RPMI 1640 media (Nissui Pharmaceutical, Tokyo, Japan) containing 10% fetal bovine serum (FBS) (Thermo Fisher Scientific, Waltham, MA, USA), penicillin (50 U/mL), streptomycin (50 μg/mL), sodium pyruvate (1 mmol/L) (Life Technologies, Carlsbad, CA, USA), HEPES buffer (10 mmol/L) (Sigma-Aldrich) and sodium bicarbonate (0.075%) (Nissui Pharmaceutical). To passage cells, podocytes were grown under permissive conditions (33 °C in the

presence of interferon-gamma (IFN-γ, 50 U/mL)). For podocytes to acquire differentiation and quiescence, resembling the *in vivo* phenotype, cells were grown under restrictive conditions at 37 °C in 95% air/5% CO_2 without IFN-γ for longer than 11 days. All experiments were performed utilizing podocytes under growth-restricted, differentiated conditions.

Western blot analysis and immunoprecipitation

For western blot analysis, cultured cells or isolated glomeruli were lysed by the addition of lysis buffer containing 50 mM Tris-buffer (pH8.0), 100 mM NaCl, 5 mM EDTA, 1% NP40, and 1% Triton X-100. Protein concentration was measured with a DC protein kit (Bio-Rad Laboratories). SDS sample buffer containing 0.35 M Tris-HCl (pH 6.8), 10% SDS, 36% glycerol, 5% β-mercaptoethanol, and 0.012% bromophenol blue was added to the lysate. Cytoplasmic or nuclear extract of the cells was obtained using an NE-PER Nuclear and Cytoplasmic Extraction Kit (Thermo Fisher Scientific, Waltham, MA, USA), and the SDS sample buffer was added to the extract solution. The proteins were separated by 8% or 12% SDS-polyacrylamide gels. After electrophoresis, the proteins were transferred onto a polyvinylidene difluoride (PVDF) transfer membrane (GE Healthcare, Buckinghamshire, England, UK) in a Tris-glycine transfer buffer (48 mM Tris-buffer, 39 mM glycine, 0.05% SDS, 10% methanol). Membranes were incubated in primary and secondary antibodies, and an ECL Plus Western blotting system (GE Healthcare, Buckinghamshire, England, UK) was used for detec-

tion. Reproducibility was confirmed in at least three independent experiments, and representative data are presented in the figures. The intensity of bands was quantified using the NIH Image J software (National Institutes of Health, Bethesda, MD, USA).

For immunoprecipitation, the cells were lysed by Triton cell lysis buffer containing 1 M Tris-buffer (pH7.4), 100 mM NaCl, 5 mM EDTA, 10 mM sodium pyrophosphate (Sigma-Aldrich), 200 μM, Na_3VO_4 (Wako Pure Chemical Industries), and 1% Triton X-100. A 1-ml cell extract containing 300- 400 μg protein was incubated with 5-10 μg target antibody or control IgG overnight at 4 °C, and subsequently incubated with 30 μg protein G sepharose (GE Healthcare) for 2 h at 4 °C. Proteins bound to the beads were eluted by boiling at 95 °C for 5 minutes, and the extract solution was used for Western blot analysis.

Immunocytochemistry

In experiments using SIRT1 inhibitors, podocytes were incubated in media with EX-527 (100 μM), cambinol (50 μM), nicotinamide (10 mM) or vehicle (ethanol) for 24 h. The media was then exchanged with media containing H_2O_2 (300 μM) or vehicle and incubation was continued for 24 h to expose cells to mild oxidative stress. In experiments using the SIRT1 activator resveratrol, podocytes were incubated in media with resveratrol (200 μM) for 3 h, then incubated in media with H_2O_2 (700 μM) for 1 h to cause strong oxidative stress.

13

To assess actin fibers and cellular morphology, cells were fixed in 4% paraformaldehyde solution, permeabilized in 0.3% Triton X solution, and incubated with Alexa Fluor 488 phalloidin (1:40 dilution) in darkness. To detect other molecules, fixed and permeabilized cells were incubated with primary antibody for 12 h and subsequently incubated with fluorescence-conjugated secondary antibody for 1 h in darkness. A BZ-9000 fluorescence microscope (Keyence, Osaka, Japan) was used for observation.

Scratch assay

Podocytes were seeded and differentiated in six-well plates. Each well was scratched with a sterile 200-µl pipette tip and incubated in medium with an SIRT1 inhibitor or vehicle (ethanol). After 3 days' incubation, the migration of cells in each stimulation group was observed. Cells were photographed under phase-contrast microscopy on days 0 and 3 after scratching, and the number of cells migrated into the scratched area was counted. The results were confirmed by three independent experiments for each SIRT1 inhibitor.

Statistical analysis

All data are reported as means ± SE. Data for two groups were analyzed with Student's t-test, and

those for more than two groups were compared by analysis of variance with Bonferroni's post hoc

test. Differences with a p value of <0.05 were considered significant. GraphPad Prism software ver-

sion 5.04 for Windows (GraphPad Software, San Diego, CA, USA) was used for data analysis.

Study approval

All animal procedures were conducted in accordance with the guidelines for the care and use of la-

boratory animals approved by the University of Tokyo School of Medicine (M-P12-66).

Results

Glomerular injury induced by anti-GBM antibody is significantly exacerbated in podocyte-specific SIRT1[pod-/-] mice.

In this study, I used podocyte-specific *Sirt1* knockout (SIRT1[pod-/-]) mice, established by crossing *Sirt1*[flox/flox] mice with podocin-Cre mice, to investigate the function of SIRT1 in podocytes. SIRT1 deletion in SIRT1[pod-/-] mice was confirmed by western blot analysis utilizing isolated glomeruli from SIRT1[pod-/-] and wild-type mice (Figure 1A). Data for blood urea nitrogen (BUN) (23.91±0.83 mg/dl in wild-type mice and 25.98±0.89 mg/dl in SIRT1[pod-/-] mice), urinary albumin creatinine ratio (U-alb/cre, 0.43±0.06 in wild-type mice and 0.53±0.08 in SIRT1[pod-/-] mice), and other physiological variables did not differ between SIRT1[pod-/-] and wild-type mice (Figure 1B, 1C, Table 1). Further, I observed no histological changes in the kidney of SIRT1[pod-/-] mice on Periodic acid-Schiff (PAS) staining (Figure 1D, 1E).

I then induced glomerular damage by injection of sheep anti-GBM antibody (anti-GBM glomerulonephritis) in SIRT1[pod-/-] and wild-type mice. Seven days after disease induction, the ratio of damaged glomeruli was significantly higher in SIRT1[pod-/-] mice (Figure 1D, 1E). Both U-alb/cre (35.76±4.87 in wild-type mice vs. 86.85±18.44 in SIRT1[pod-/-] mice) and BUN (22.10±0.97 mg/dl in wild-type mice vs. 25.88±1.05 mg/dl in SIRT1[pod-/-] mice) were also significantly exacerbated in

SIRT1$^{\text{pod-/-}}$ mice compared with wild-type mice (Figure 1F, 1G). I confirmed that the level of binding of anti-GBM antibodies to glomeruli in the two groups was similar (Figure 1H). Because the podocyte-specific deletion of SIRT1 induced glomerular vulnerability, I then focused on the critical function of SIRT1 in the maintenance of podocyte homeostasis and subsequent glomerular function and structure.

Table1. Physiological data of the experimental mice.

	SIRT1^{+/+}	SIRT1[pod-/-]	p value
n	24	22	–
Age (weeks)	13.96 ± 0.12	14.09 ± 0.09	0.41
Body weight (g)	26.8 ± 0.36	26.6 ± 0.62	0.28
Systolic BP (mmHg)	97.2 ± 2.9	99.3 ± 3.5	0.66
Diastolic BP (mmHg)	50.2 ± 5.5	54.83 ± 4.7	0.53
Pulse rate (bpm)	600.6 ± 45.8	608.4 ± 53.4	0.91

Data are means ± SE of wild-type mice and SIRT1[pod-/-] mice before disease induction. BP, blood pressure.
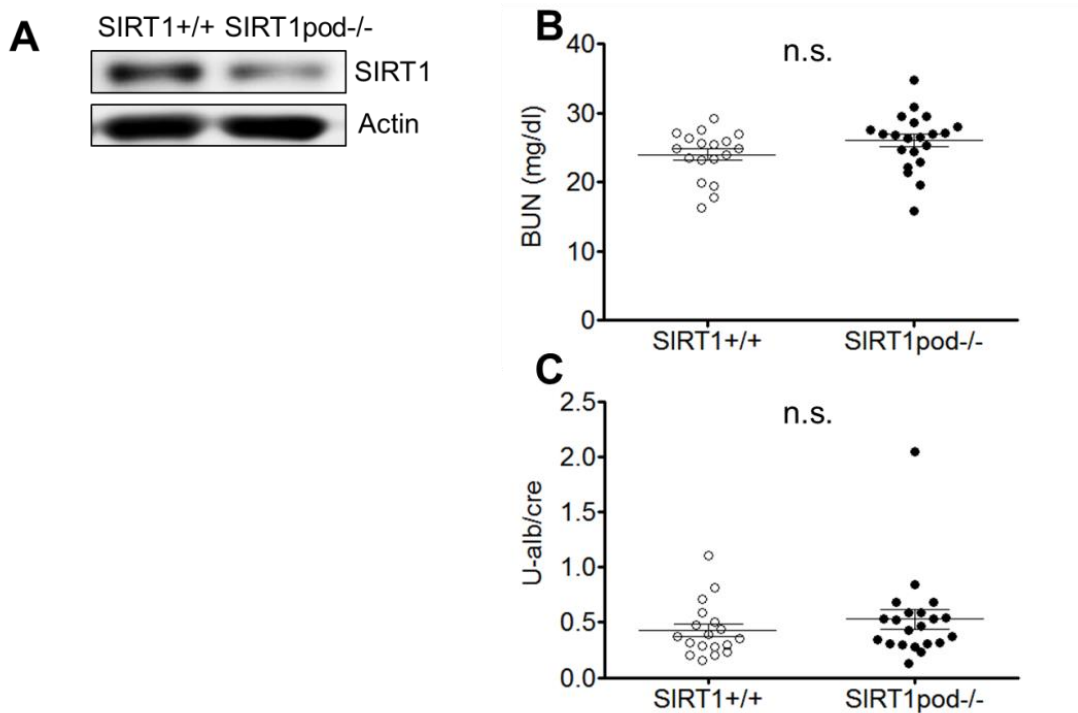
Figure 1. Glomerular injury and renal dysfunction were exacerbated in podocyte-specific *Sirt1* knockout (SIRT1[pod-/-]) mice with glomerular disease.

(A) Western blot analysis using isolated glomeruli from wild-type or SIRT1[pod-/-] mice. A reduction in SIRT1 expression in SIRT1[pod-/-] mice was confirmed. (B) Blood urea nitrogen (BUN) level of wild-type (n=18) and SIRT1[pod-/-] mice (n=21). (C) Urinary albumin per creatinine ratio of wild-type (n=18) and SIRT1[pod-/-] mice (n=21). n.s., not significant.

D

E
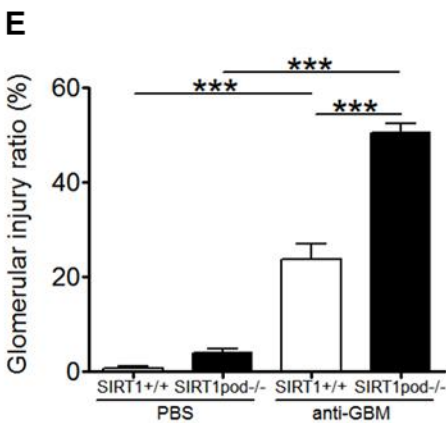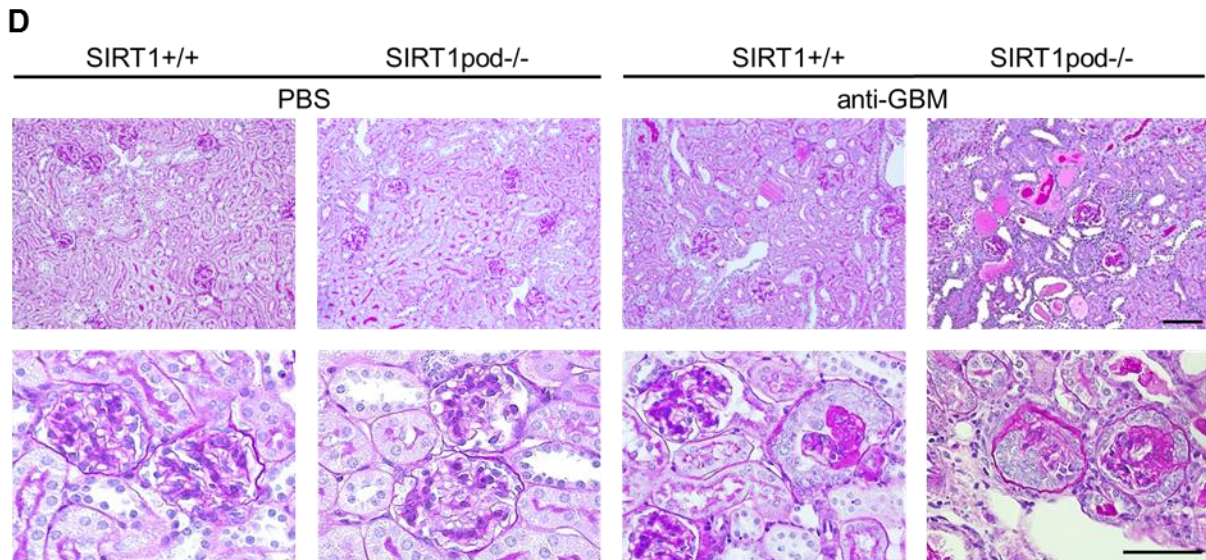
Figure 1 (cont.).

(D) Histological analysis by PAS staining. At 7 days after glomerular disease induction with anti-GBM antibody injection, glomerular damage was more severe in SIRT1[pod-/-] mice than in wild-type mice. Scale bars, 100 μm. (E) Ratio of injured glomeruli in PBS-injected wild-type (n=6) or SIRT1[pod-/-] mice (n=7) and wild-type (n=9) or SIRT1[pod-/-] mice (n=9) with anti-GBM glomerulonephritis (*** p<0.001). Glomerular damage in SIRT1[pod-/-] mice with anti-GBM glomerulonephritis was significantly worse than that in wild-type mice.
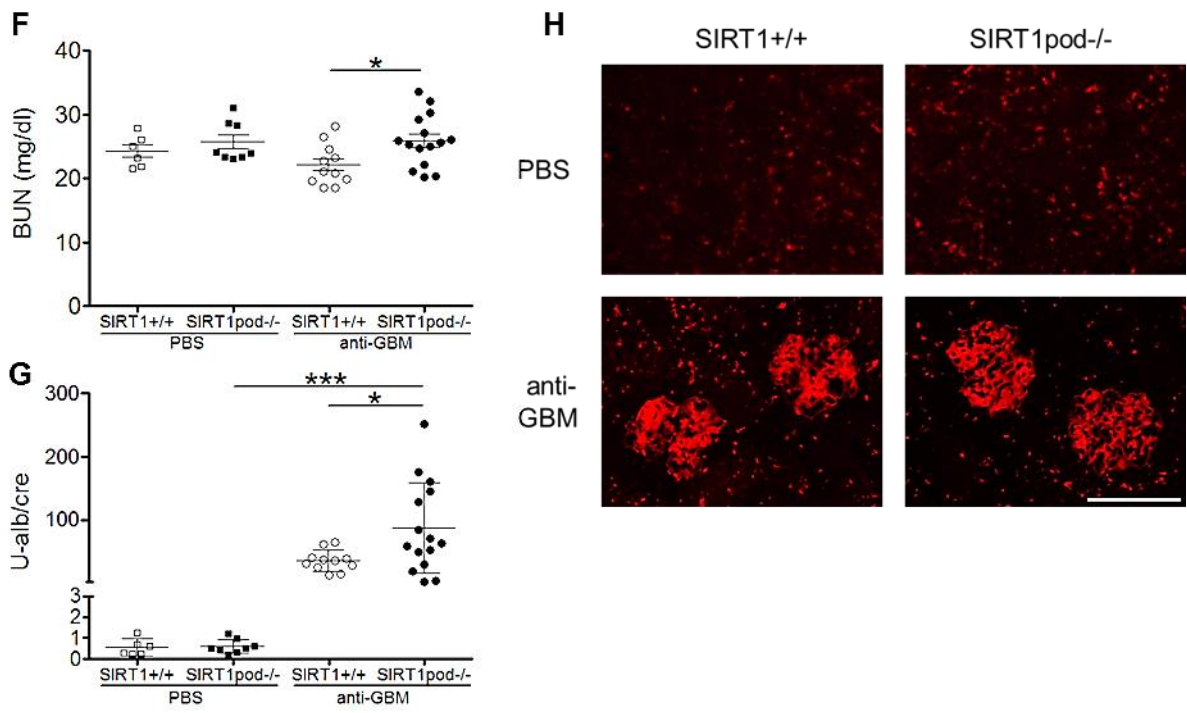
Figure 1 (cont.).

(F, G) BUN (F) or urinary albumin levels (G) in experimental mice. Seven days after anti-GBM glomerulonephritis induction, blood and urine were collected from PBS-injected wild-type (n=6) and SIRT1[pod-/-] (n=8) mice and anti-GBM glomerulonephritis-induced wild-type (n=11) and SIRT1[pod-/-] (n=15) mice. Both BUN and urinary albumin levels were significantly higher in SIRT1[pod-/-] mice than in wild-type mice under disease conditions (* p<0.05, *** p<0.001). (H) Detection of anti-GBM antibody in the glomeruli of experimental mice. Immunofluorescence analysis showed a similar level of anti-GBM antibody binding to GBM in wild-type and SIRT1[pod-/-] mice, indicating disease induction in both groups was identical. Scale bars, 100 μm.

Podocyte injury is exacerbated by deficiency of podocyte SIRT1 expression in anti-GBM glomerulonephritis.

I next determined the effect of SIRT1 on podocyte homeostasis by assessing the change in the expression of podocyte-specific molecules. On western blot analysis using the lysate of isolated glomeruli of the mice, the expression of nephrin, synaptopodin, and Wilms tumor 1 protein (WT-1) after the induction of anti-GBM glomerulonephritis was significantly decreased in SIRT1$^{pod-/-}$ mice compared with wild-type mice (Figure 2A). I confirmed that the expression of actin was not changed and that this variable could therefore be used as an internal control by comparison with the expression of α-tubulin (Figure 2A). Immunofluorescent studies showed that SIRT1$^{pod-/-}$ and wild-type mice had similar synaptopodin and WT-1 expression before disease induction and decreased expression after induction, but that this decrease was greater in SIRT1$^{pod-/-}$ mice (Figure 2B, 2C). These results are compatible with the exacerbation of histological and biochemical data in anti-GBM antibody-injected SIRT1$^{pod-/-}$ mice shown in Figure 1.
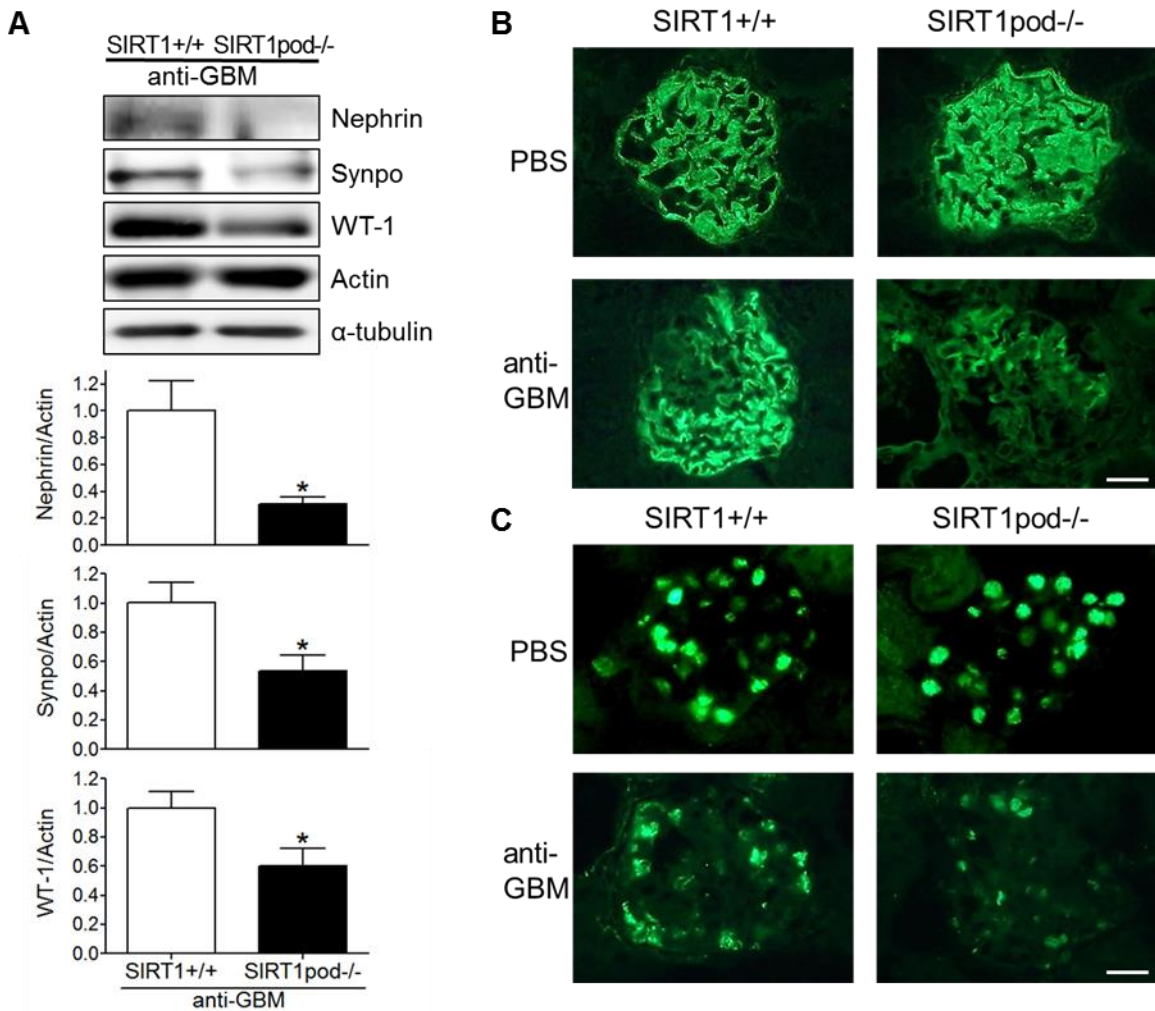
Figure 2. Podocyte slit diaphragm (SD) damage was exacerbated by SIRT1 deficiency *in vivo*.
(A) Podocyte injury level in isolated glomeruli of wild-type or podocyte-specific *Sirt1* knockout (SIRT1[pod-/-]) mice at 7 days after anti-GBM glomerulonephritis induction. Western blot analysis followed by densitometry was performed to assess podocyte injury level, as estimated by the expression of SD-related proteins such as nephrin, synaptopodin (Synpo), and WT-1. For densitometry, actin was used as an internal control. α-Tubulin expression was also assessed to confirm that the expression of actin was not changed in SIRT1-deficient podocytes. Expression of these SD-related proteins was significantly reduced in SIRT1[pod-/-] mice compared with wild-type mice (* $p<0.05$). (B, C) Representative immunohistochemical pictures of synaptopodin (B) or WT-1(C) in experimental mice. Decreased SD-related protein expression was severe in anti-GBM glomerulonephritis-induced SIRT1[pod-/-] mice compared with wild-type mice. Scale bars, 20 μm.

Foot process effacement and actin fiber derangement are exacerbated by podocyte-specific

***Sirt1* knockout.**

To elucidate the mechanism by which SIRT1 deficiency deranges podocyte homeostasis in podocytes, I evaluated structural alterations in podocytes in SIRT1$^{pod-/-}$ mice by electron microscopy. Following anti-GBM antibody injection, foot process effacement was more widespread and more severe in SIRT1$^{pod-/-}$ than in wild-type mice, and the accumulation of actin fibers, which indicates actin cytoskeleton derangement, was higher (Figure 3). These findings are consistent with the marked increase in albuminuria in SIRT1$^{pod-/-}$ mice with anti-GBM glomerulonephritis (Figure 1G). These results suggest that the major features of podocyte vulnerability following *Sirt1* knockout were disruption of the actin cytoskeleton and slit diaphragm, and that these lead to the exacerbation of glomerular injury.
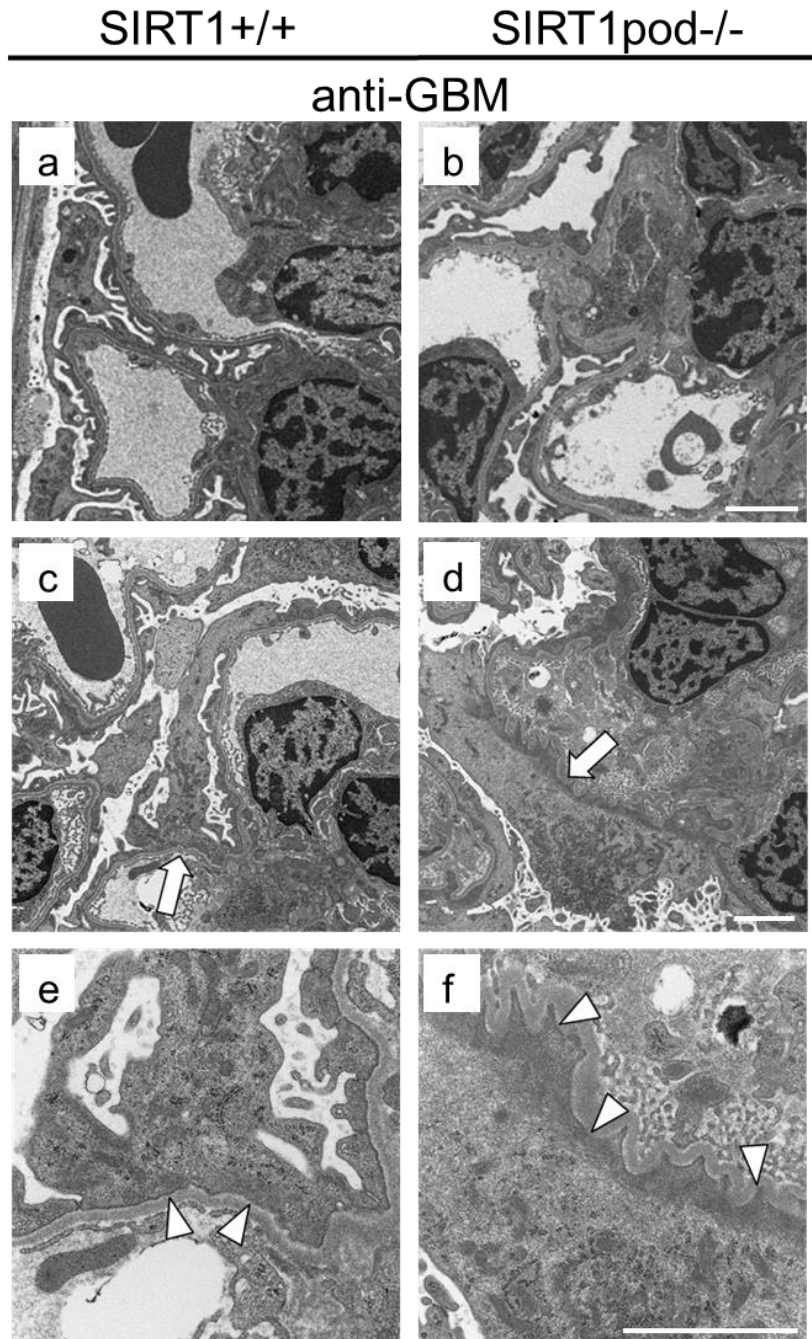
Figure 3. Foot process effacement and disruption of actin cytoskeleton were exacerbated in podocyte-specific *Sirt1* knockout (SIRT1[pod-/-]) mice.

Electron microscopic images of glomeruli of anti-GBM glomerulonephritis-induced wild-type (a, c, e) and SIRT1[pod-/-] (b, d, f) mice. In SIRT1[pod-/-] mice, foot process effacement was severe (b) compared with that in wild-type mice (a). The lower panels (e and f) are enlargements of the parts indicated by arrows in the middle panels (c and d). Actin fiber accumulation (arrow heads) was also increased by SIRT1 deficiency in podocytes. Scale bars, 2 μm.

SIRT1 activity is necessary for maintenance of actin cytoskeleton in cultured podocytes

To assess the effect of SIRT1 on actin fiber dynamics, I investigated structural changes in cultured murine podocytes treated with or without SIRT1 inhibitors. I used hydrogen peroxide (H_2O_2) to induce cellular damage in *in vitro* experiments on the basis that oxidative stress, estimated by nitrotyrosine staining, was significantly induced in glomerular cells, including podocytes, of anti-GBM glomerulonephritis mice (Figure 4A). The cultured podocytes were pretreated with the SIRT1 inhibitor EX-527 (100 μM) or vehicle (ethanol) for 24 h, incubated with or without H_2O_2 (300 μM) for 24 h, then stained for actin fiber using Alexa Fluor 488 phalloidin. The SIRT1 inhibitory effect of EX-527 was confirmed by western blot analysis for acetyl-histone H3 (Figure 4B). While mild derangement of actin cytoskeleton was seen in the podocytes treated with either H_2O_2 or EX527, severe derangement was seen in SIRT1-inactived podocytes treated with H_2O_2 (Figure 4C). Similar results were observed in experiments using other SIRT1 inhibitors such as cambinol or nicotinamide (NAM) instead of EX-527 (Figure 4C). These results suggest that SIRT1 activity is necessary for the maintenance of actin fiber.

I next confirmed the effect of SIRT1 on maintenance of actin cytoskeleton using resveratrol, a SIRT1 activator. Pretreatment with resveratrol (200 μM) prevented the derangement induced in cultured podocytes by a high concentration of H_2O_2 (700 μM) (Figure 4D). I confirmed that a change in SIRT1 activity did not influence the expression of actin by western blot analysis in comparison with α-tubulin (Figure 4A). These loss-of- and gain-of-function analyses revealed that SIRT1 function is

associated with maintenance of the actin cytoskeleton.
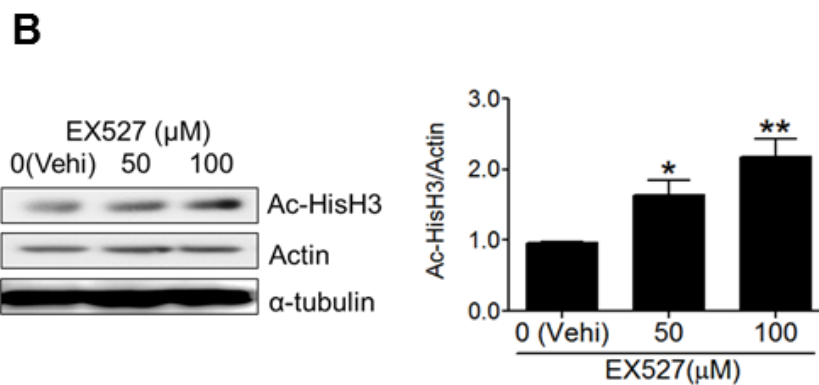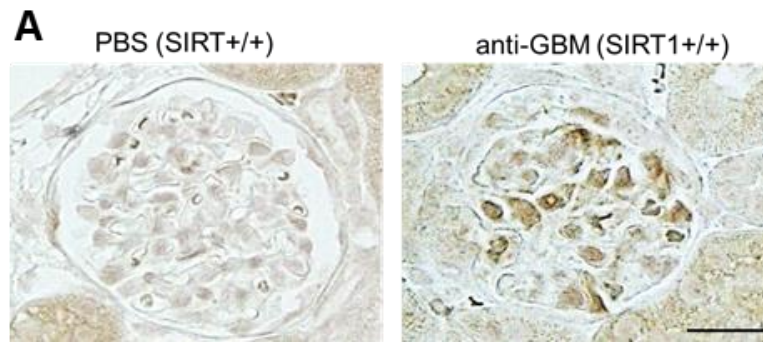
Figure 4. SIRT1 activity was necessary for actin cytoskeleton maintenance in podocytes.
(A) Oxidative stress detection by immunohistochemistry for nitrotyrosine in glomeruli of control or anti-GBM glomerulonephritis-induced mice. In anti-GBM antibody-injected mice, podocytes were positive for nitrotyrosine, indicating that oxidative stress was induced by anti-GBM glomerulone-phritis. Scale bar, 50 μm. (B) Western blot analysis and densitometry for acetyl-histone H3 (Ac-HisH3) in cultured podocytes (* $p<0.05$, ** $p<0.01$). EX527, a SIRT1 inhibitor, significantly increased acetylation level of histone H3 in a dose-dependent manner in podocytes.
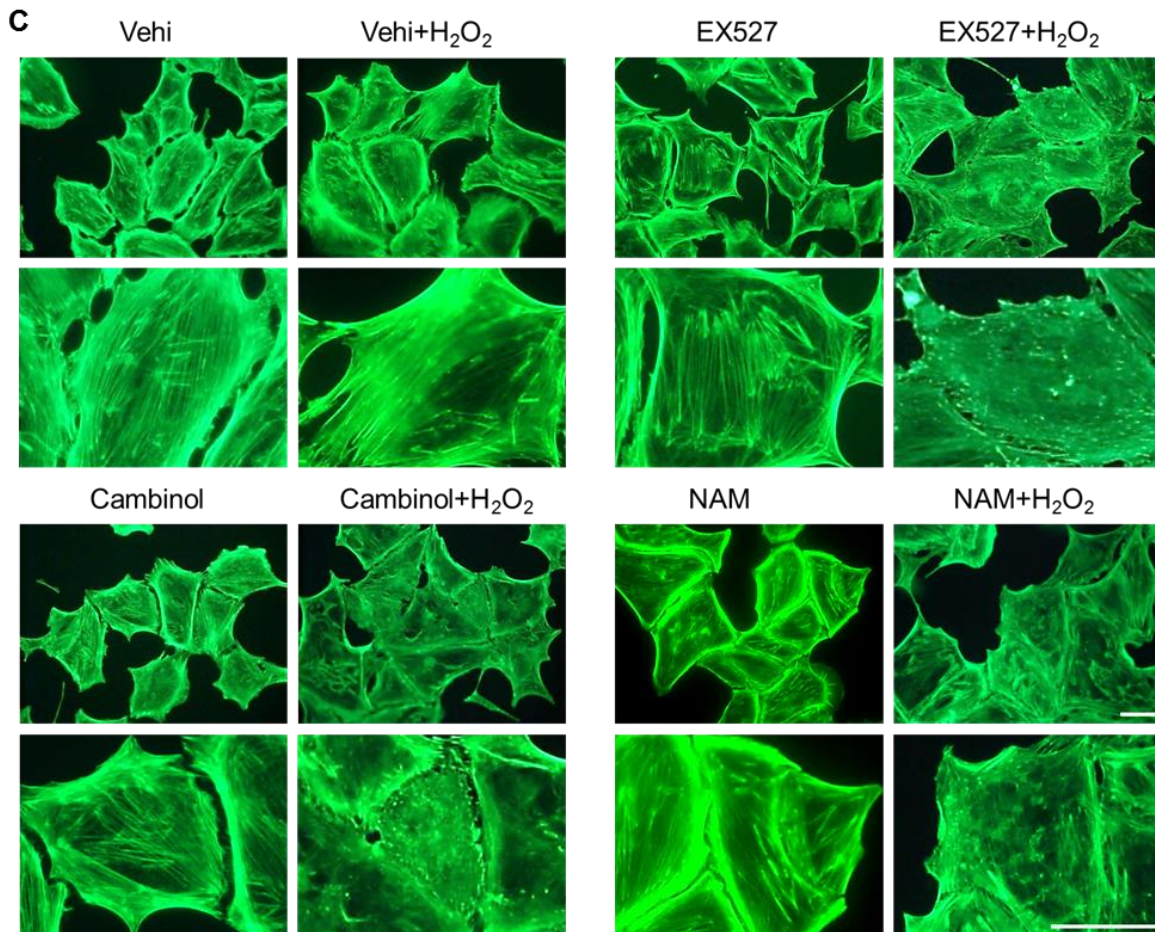
Figure 4 (cont.).

(C) Detection of actin fiber by fluorescein-phalloidin staining in cultured podocytes. Lower panels are enlargements. Cultured podocytes were treated with SIRT1 inhibitors (EX527, 100 μM; cambinol, 50 μM; or nicotinamide (NAM), 10 mM) or vehicle (Vehi, ethanol) for 24 h and then treated with or without H_2O_2 (300 μM) for 24 h. H_2O_2 was used to induce podocyte injury to mimic that in anti-GBM glomerulonephritis. Actin cytoskeleton derangement was markedly deteriorated in podocytes treated with both EX527 and H_2O_2 compared with the cells treated with either EX527 or H_2O_2. Similar results were confirmed using the other SIRT1 inhibitors cambinol or NAM. Scale bars, 50 μm.

D
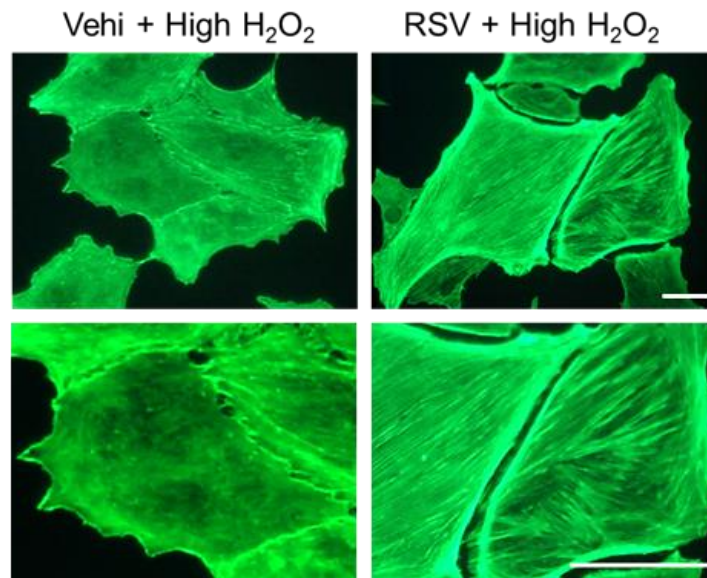
Figure 4 (cont.).

(D) Fluorescein-phalloidin staining of cultured podocytes treated with SIRT1 activator under oxidative stress conditions. Lower pictures are enlargements. Cultured podocytes were pretreated with SIRT1 activator resveratrol (RSV, 200 mM) or vehicle (Vehi, ethanol) for 3 h, then cultured with high dose H_2O_2 (High H_2O_2, 700 μM) for 1 h. RSV prevented actin cytoskeleton derangement induced by oxidative stress. Scale bars, 50 μm.

Podocyte motility is reduced by SIRT1 inhibition.

Because the cellular motility of podocytes is dependent on their dynamic assembly of actin [40–43], I hypothesized that podocyte migration ability is attenuated when the actin fibers are disrupted by SIRT1 inhibition. To address this, I examined the change in cellular motility by scratch assay utilizing cultured podocytes. Motility was markedly reduced by EX-527 treatment compared with vehicle (Figure 5A). Similar results were observed using other SIRT1 inhibitors (Figure 5B, 5C). These findings suggest that SIRT1 activity plays an essential role in actin fiber dynamics.
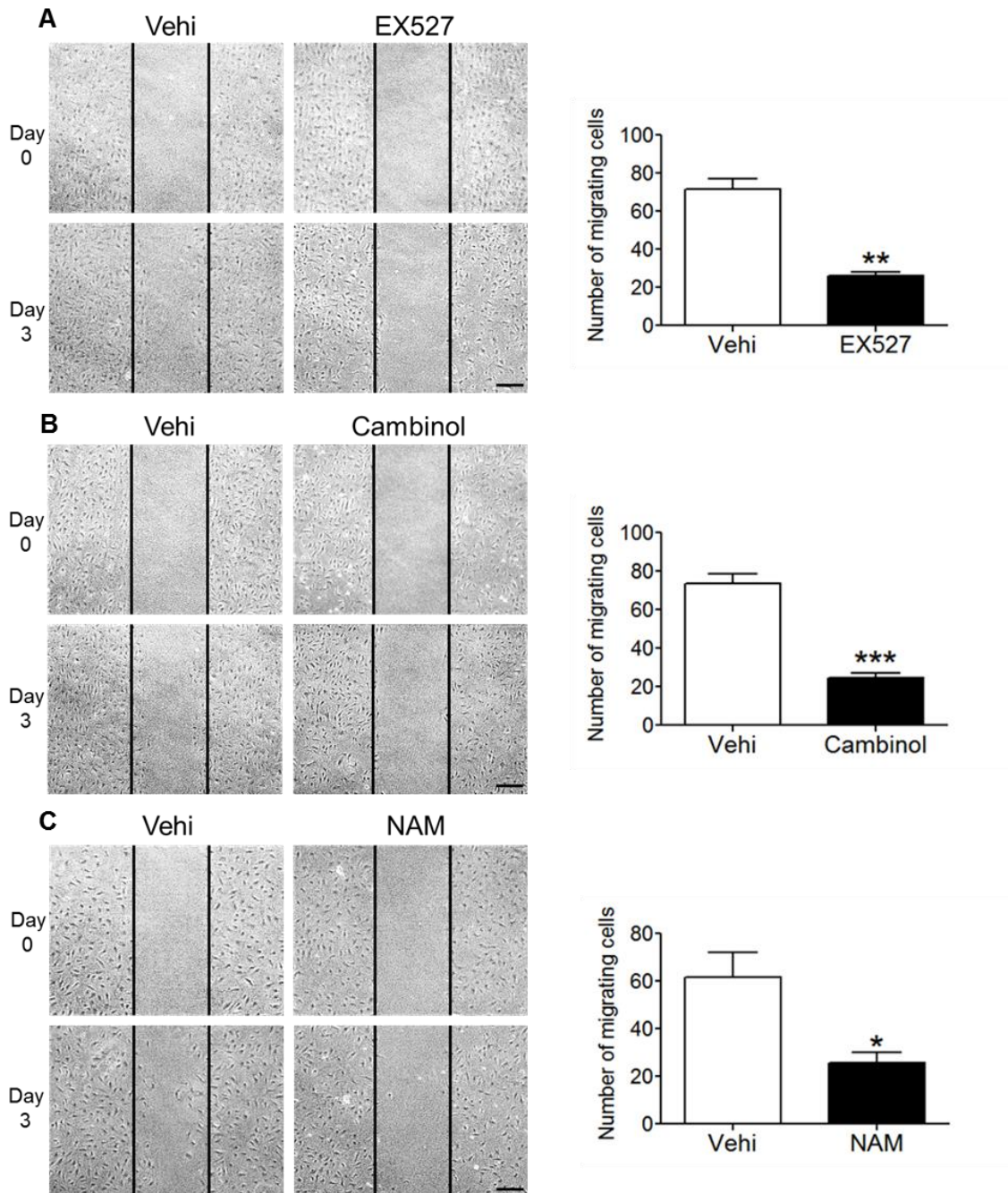
Figure 5. SIRT1 activity contributed to podocyte motility.

SIRT1 activity contributed to podocyte motility. Scratch assay followed by counting of migrated podocytes treated with the SIRT1 inhibitions EX527 (A), cambinol (B), or nicotinamide (C). The cells were cultured with 100 μM EX527, 50 μM cambinol, or 5 mM nicotinamide (NAM) for 3 days after scratch, and then the number of migrated cells was counted. Inhibition of SIRT1 activity significantly retarded podocyte migration (* $p < 0.05$, ** $p < 0.01$, *** $p < 0.001$). Results were confirmed by three independent experiments. Scale bars, 200 μm.

**SIRT1 deacetylates cortactin in nuclei of podocytes**

Cortactin, an actin-associated protein, interacts with actin fibers, and polymerizes and stabilizes them [40], [44] (Figure 7S). Some reports demonstrated that the acetylation state of cortactin contributes to the cell motility and mobility of cancer cells [44–46]. I therefore investigated the effect of SIRT1 on the acetylation state of cortactin and subsequent actin cytoskeleton maintenance and dynamics in podocytes. On western blot analysis, the ratio of acetylated cortactin to total cortactin was increased in cultured podocytes treated with SIRT1 inhibitors in a dose-dependent manner (Figure 6A, 6B). Conversely, this ratio was reduced in resveratrol-treated podocytes (Figure 6C). Moreover, these *in vitro* data were consistent with an *in vivo* study demonstrating that the level of acetylated cortactin in isolated glomeruli from SIRT1$^{pod-/-}$ mice was significantly high compared to that in wild-type mice (Figure 6D). This interaction between SIRT1 and cortactin was confirmed in immunoprecipitation analysis in cultured podocytes (Figure 6E) and in immunofluorescence analysis, which showed that SIRT1 was colocalized with cortactin in nuclei (Figure 6F). These data suggest that SIRT1 deacetylates cortactin in the nuclei of podocytes and maintains of actin cytoskeleton, resulting in podocyte homeostasis.
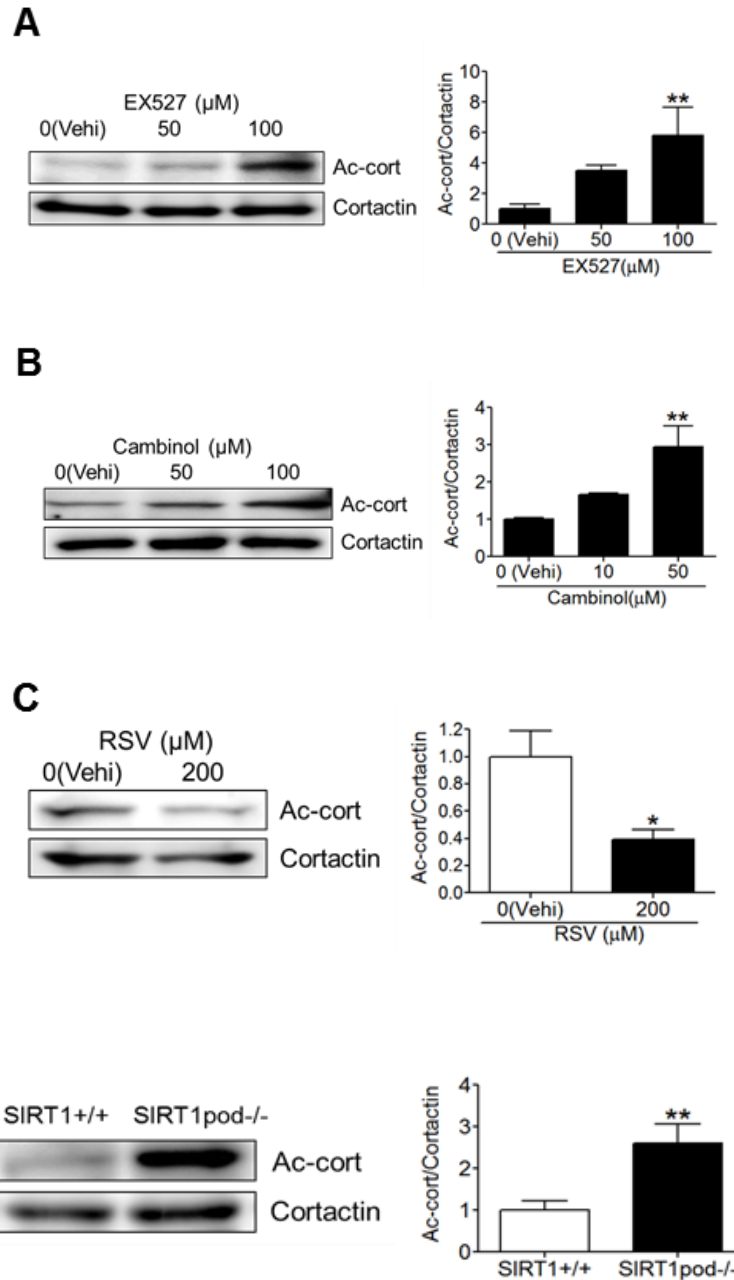
Figure 6. SIRT1 regulated cortactin acetylation *in vitro* and *in vivo*.
(A, B, C) Western blot analysis of acetylated cortactin (Ac-cort) and total cortactin in the whole cell extract of cultured podocytes treated with the SIRT1 inhibitors EX527 (A) or cambinol (B), or the SIRT1 activator resveratrol (RSV, C). Right panels show quantitative analyses of the ratio of Ac-cort to cortactin (* $p<0.05$, ** $p<0.01$). The ratio of Ac-cort was significantly increased by EX527 or cambinol in a dose-dependent manner, whereas it was decreased by RSV. (D) Western blot analysis of Ac-cort and total cortactin in the isolated glomeruli of wild-type or SIRT1[pod-/-] mice. Quantitative analysis of the ratio of Ac-cort to cortactin is shown in the right panel (** $p<0.01$). The ratio of Ac-cort was significantly increased in SIRT1[pod-/-] mice compared with wild-type mice.
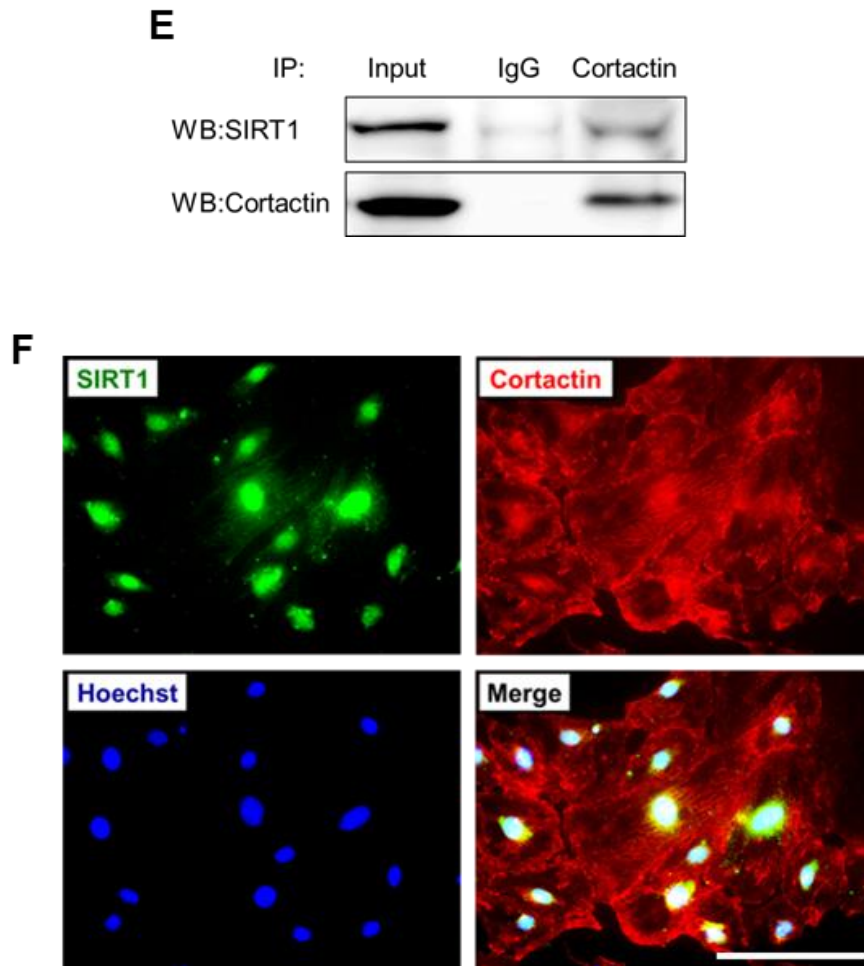
Figure 6 (cont.).

(E) Immunoprecipitation analysis for the detection of SIRT1 binding with cortactin. Whole-cell extract of cultured podocytes without stimulation was immunoprecipitated with anti-cortactin antibody or normal anti-rabbit IgG, and the precipitate was analyzed by western blot analysis using anti-SIRT1 or anti-cortactin antibodies. A protein sample without immunoprecipitation was also analyzed (input) as a control. The results showed that SIRT1 interacts with cortactin. (F) Immunofluorescence analysis for detection of SIRT1 and cortactin in cultured podocytes. Staining of SIRT1, cortactin, nuclei (Hoechst33258) and a merged image are shown. The merged figure shows that SIRT1 was colocalized with cortactin in the nuclei, suggesting that SIRT1 colocalizes with cortactin in the nuclei. Scale bar, 100 μm.

SIRT1 regulates actin cytoskeleton dynamics via acetylation of cortactin in podocytes.

Finally, I investigated the change in cortactin localization by acetylation and its contribution to actin cytoskeleton maintenance and dynamics. Immunocytochemistry demonstrated that total (acetylated and deacetylated) cortactin was localized both in the cytoplasm and nucleus, and that the cytoplasmic cortactin was partly colocalized with actin fibers. When actin cytoskeleton derangement was induced by H_2O_2 in cells treated with EX527, the fiber-like distribution of cytoplasmic cortactin was simultaneously disrupted, and cortactin was dissociated from actin fiber (Figure 7A, 7B). In contrast to total cortactin, acetylated cortactin was localized only in the nucleus, and remained colocalized with SIRT1 regardless of the state of actin cytoskeleton (Figure 8A, 8B). I confirmed the localization of acetylated cortactin in podocytes *in vivo* (Figure 8C). Taking these findings together, I speculated that the deacetylation of cortactin by SIRT1 regulates the interaction with actin fibers.

   I then assessed the effect of SIRT1 on the acetylation level of cortactin in the cytoplasm and nucleus of cultured podocytes. In nuclear extract, acetylated cortactin was increased by SIRT1 inhibition, as observed in the experiments using whole cell lysate, whereas acetylated cortactin was not detected in cytoplasmic extract (Figure 8D, 8E). Furthermore, the nuclear cortactin level was increased, while that of cytoplasmic cortactin was conversely decreased (Figure 8D, 8E). These results suggest that cortactin is predominantly deacetylated by SIRT1 in the nucleus, and that deacetylated cortactin is transported from the nucleus to the cytoplasm, where it maintains actin cytoskeleton. The

deacetylation activity of SIRT1 is thus necessary for cortactin function and its transport from the nucleus to cytoplasm.
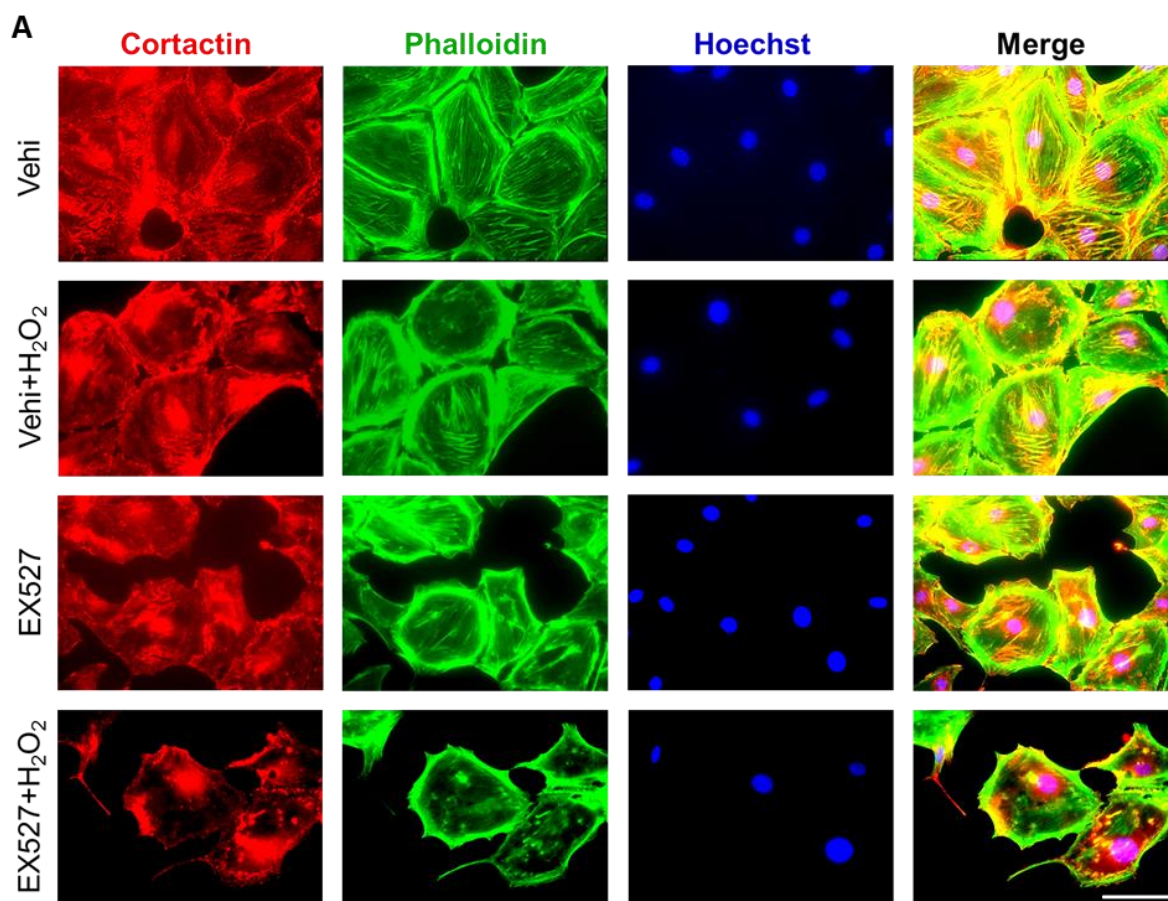
Figure 7. SIRT1 maintained actin cytoskeleton by regulation of cortactin deacetylation.
(A) Detection of cortactin by immunofluorescence in cultured podocytes treated with SIRT1 inhibitor under oxidative stress. Staining of cortactin, actin fibers (phalloidin), nuclei (Hoechst33258), and their merged image are shown. Cultured podocytes were treated with vehicle (Vehi, ethanol) or EX527 (SIRT1 inhibitor, 100 μM) for 24 h, and subsequently incubated for 24 h with or without H_2O_2 (300 μM). In vehicle treated-cells cortactin was observed in both cytoplasm and nucleus, and cytoplasmic cortactin was partly colocalized with actin fibers. Cells treated with either H_2O_2 or EX527 showed moderate actin cytoskeleton derangement and partial disruption of the fiber-like distribution of cortactin. Treatment with both EX527 and H_2O_2, namely inhibition of SIRT1 activity under oxidative stress conditions, produced severe derangement of actin cytoskeleton and the apparent absence of fiber-like distribution of cytoplasmic cortactin; in contrast, no changes in nuclear cortactin were observed. Scale bar, 100 μm.

B

H₂O₂ (-) H₂O₂ (+)

Vehi

EX527
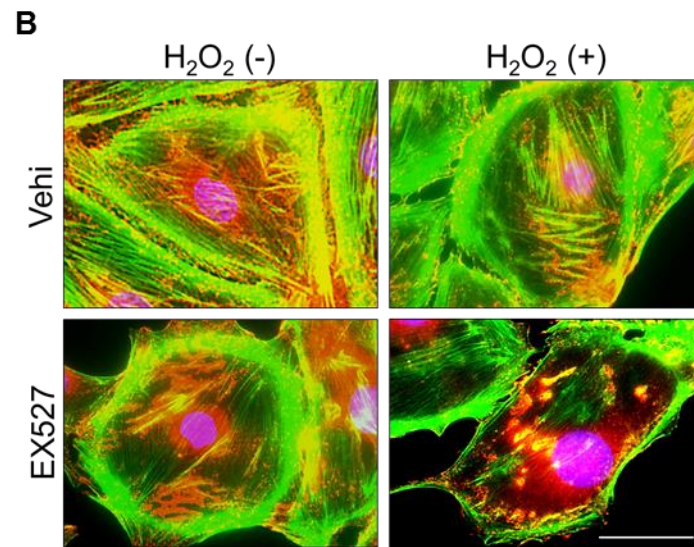
Figure7 (cont.).

(B) Enlargements of the merged images shown in (A). Actin cytoskeleton derangement associated with the disruption of fiber-like distribution of cytoplasmic cortactin is clearly observed in SIRT1-inhibited podocytes under oxidative stress conditions. Scale bar, 50 µm.
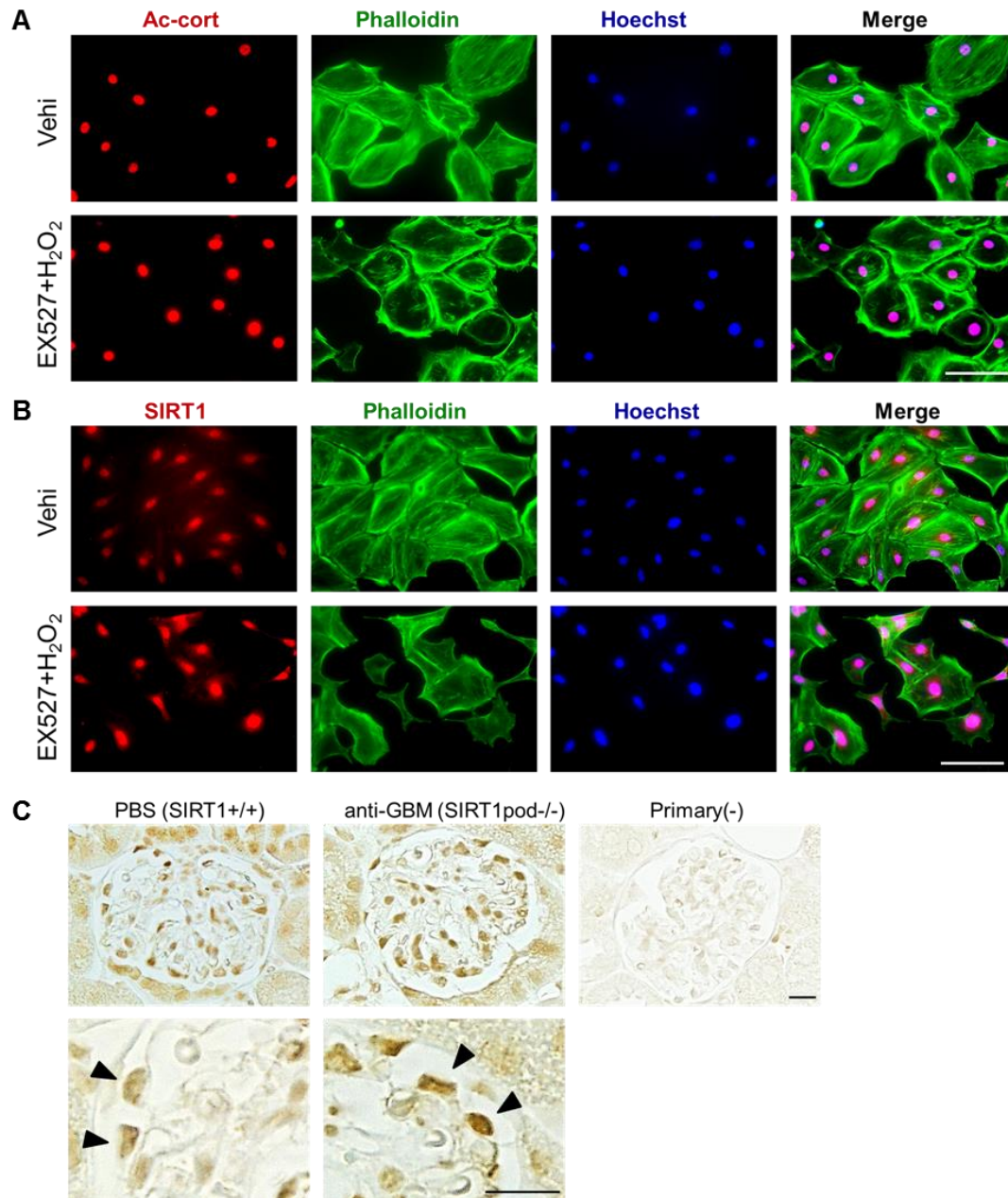
Figure 8. SIRT1 deacetylated cortactin in the nuclei of podocytes.

(A, B) Detection of acetyl-cortactin (A) and SIRT1 (B) by immunofluorescence in cultured podocytes treated with SIRT1 inhibitor under oxidative stress. Cultured podocytes were analyzed for staining of acetyl-cortactin (Ac-cort) (A) or SIRT1 (B), with actin fiber (phalloidin) and nuclei (Hoechst 33258). Acetylated cortactin was observed only in nuclei regardless of the state of actin cytoskeleton in association with colocalization of SIRT1. Scale bar, 100 μm. (C) Immunostaining of acetyl-cortactin in the kidney of PBS-injected wild-type and anti-GBM glomerulonephritis-induced SIRT1^pod-/- mice. Lower images are enlargements focusing on podocytes (arrow heads). In the podocytes, acetyl-cortactin was detected only in nuclei in both mice, which was compatible with the results *in vitro* shown in (A). Scale bars, 20 μm.

D

E
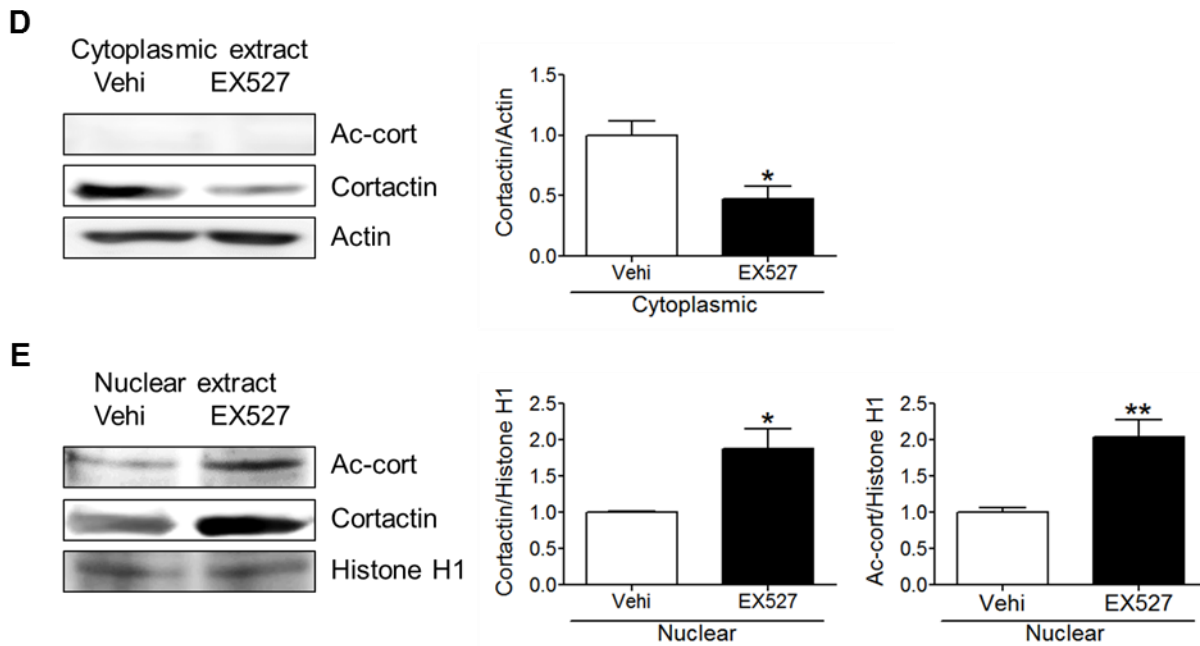
Figure8 (cont.).

(D, E) Detection of cortactin by western blot analysis using the cytoplasmic (D) or nuclear extract (E) of cultured podocytes. Cells treated with EX527 (SIRT1 inhibitor, 100 μM) were analyzed for acetylated or total cortactin and their expression levels were quantitatively analyzed. (* $p < 0.05$, ** $p < 0.01$). Actin and histone H1 were used as internal controls of cytoplasmic and nuclear extracts, respectively. Total cortactin level in cytoplasm was reduced by SIRT1 inhibition, whereas nuclear cortactin level was conversely increased in association with nuclear accumulation of acetyl-cortactin.
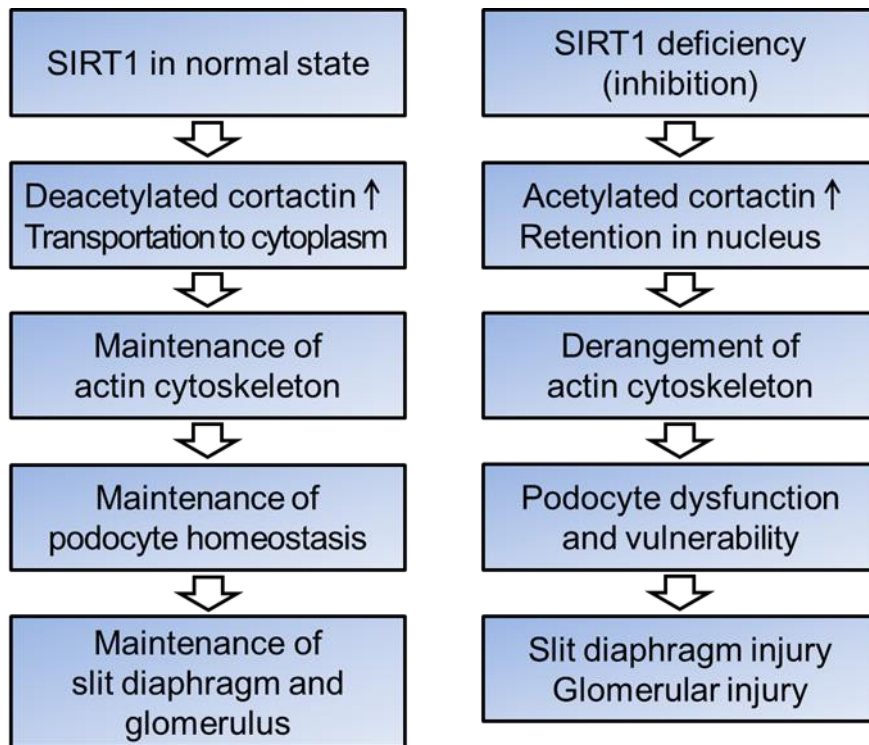
Figure 9. SIRT1 maintains podocyte homeostasis by deacetylation of cortactin.

In the normal state, SIRT1 deacetylates and activates cortactin, and the deacetylated cortactin functions for the maintenance of actin cytoskeleton in the cytoplasm, leading in turn to the maintenance of podocyte homeostasis. As a result, the glomerulus, including the slit diaphragm, is maintained. Conversely, suppression of SIRT1 induces an increase in acetylated cortactin in the nucleus and decrease in active cortactin in the cytoplasm, which leads to the derangement of actin cytoskeleton, with consequent podocyte dysfunction or podocyte vulnerability leading to slit diaphragm injury, followed by glomerular injury.

Discussion

In this study, I established SIRT1$^{pod-/-}$ mice. Podocyte-specific *Sirt1* knockout mice showed no bio-

chemical or histological abnormalities in the kidney. However, pathological alterations, such as FP

effacement and actin fiber derangement, were significantly exacerbated in the podocytes of

SIRT1$^{pod-/-}$ mice after glomerular disease induction (anti-GBM glomerulonephritis), and in cultured

podocytes with modulated SIRT1 activity under oxidative stress conditions as a mimic of anti-GBM

glomerulonephritis. Importantly, I also found that SIRT1 deacetylated cortactin, an actin fi-

ber-associated molecule, and thereby enhanced cortactin activity, with subsequent polymerization

and stabilization of actin fibers. My study reveals that SIRT1 has the novel function in podocytes of

maintaining actin cytoskeleton and subsequently the structure of SD via the deacetylation of cortac-

tin. Further, it indicates the possibility that SIRT1 is essential to the protection of podocyte function

as well as structure against pathogenic microenvironments, such as oxidative stress. My results

therefore clarify the novel beneficial effect of SIRT1 on podocyte homeostasis.

The cytoskeletal element of FP is composed of actin fibers only, indicating that actin fibers are es-

sential to maintenance of the structure and function of SD [47]. Mutations of actin fiber binding pro-

teins, such as α-actinin-4 or CD2AP, lead to podocyte injury owing to disorganization of the actin

cytoskeleton and disruption of its filtration barrier [43], [48], [49]. I performed a scratch assay and

showed that SIRT1 was necessary for podocyte motility. Although the question of whether motile

podocytes induce proteinuria and renal damage is still controversial [8], [43], it is widely accepted that the reorganization of actin cytoskeleton is necessary for podocyte migration [42], [43], [50]. Thus, the results of my experiments show that SIRT1 is required for the appropriate reorganization of actin cytoskeleton in podocytes.

SIRT1 belongs to the HDAC family, which acts to deacetylate proteins and histones, and controls epigenetic changes and protein functions [9], [51–54]. SIRT1 contributes to the regulation of pathogenic intracellular signaling in podocytes. Chuang and colleagues demonstrated that SIRT1 overexpression in cultured murine podocytes prevents glycative stress-induced apoptosis under diabetic conditions [35], while Yuan and colleagues showed that SIRT1 prevents aldosterone-induced mitochondrial dysfunction and the subsequent apoptosis of podocytes [36]. Both studies highlight the link between the podocyte-protective effect of SIRT1 and podocyte apoptosis. I directly verified the function of SIRT1 in podocytes using novel genetically engineered podocyte-specific knockout mice, and elucidated the underlying mechanisms for this phenomenon *in vivo* using pharmacological methods in cultured podocytes *in vitro*. My results revealed a novel function of SIRT1 in podocytes: SIRT1, particularly its deacetylase activity against cortactin, protects podocyte homeostasis via the maintenance of actin cytoskeleton. My experiments therefore directly reveal for the first time the functional role and biological mechanism of SIRT1 expressed in podocytes.

Cortactin is an actin filament-binding substrate of Src tyrosine kinase [55], [56] which regulates the assembly, polymerization, and stabilization of the branched actin network [45], [57–59]. Recent

papers demonstrated that deacetylation is also important in the association of cortactin with F-actin and the promotion of actin assembly and stabilization of actin fibers in cancer cells [45], [46]. These findings are consistent with my present data observed in podocytes. Although the colocalization of cortactin with actin fibers in podocytes has been reported [60], [61], the function and regulation of cortactin has remained unclear. My present study revealed that the suppression of SIRT1 expression under pathogenic conditions, such as oxidative stress-related podocyte injury, induced the derangement of actin cytoskeleton via the acetylation of cortactin, indicating a critical link between SIRT1 and cortactin in podocyte homeostasis.

Another novel finding of my study was that SIRT1 is required for the nuclear-cytoplasmic shuttle of cortactin in podocytes. I assessed changes in the amount of total or acetylated cortactin in the cytoplasm and nuclei of glomeruli of SIRT[pod-/-] mice and of cultured podocytes with modulated SIRT1 activity. Acetylated cortactin was mainly detected in the nuclei and its level was inversely correlated with SIRT1 activity. Considered together with the finding that SIRT1 is coprecipitated with cortactin, it is likely that SIRT1 is necessary for the transport of cortactin from nucleus to cytoplasm. The regulatory role of posttranslational acetylation on the nuclear import and export of proteins is well known [62]. In particular, nuclear protein LKB1 is exported to the cytoplasm following deacetylation by SIRT1 [63]. Based on these findings, my results strongly suggest that SIRT1 regulates cortactin localization by deacetylation.

In this study, I investigated the alteration of kidney of SIRT1pod-/- mice after glomerular disease

induction by anti-GBM antibody. From other viewpoints, considering that *Sirt1* is deeply associated with longevity, it is possible that these knockout mice without any stimulation show glomerular injury or albuminuria in an advanced age such as 1 or 2 year-old. I should investigate whether some kind of injuries are induced in aged SIRT1$^{pod-/-}$ mice. Moreover, the various role of *Sirt1* includes regulation of inflammation. I examined the macrophage infiltration to glomeruli in glomerular damage-induced SIRT1$^{pod-/-}$ mice and found a tendency to increase in the number of the cells compared to wild-type mice (data not shown). In anti-GBM nephritis, glomerular inflammation was certainly caused and the exacerbation of inflammatory reaction might be one of the reasons which induced more severe podocyte injury in SIRT1$^{pod-/-}$ mice. In any cases, the primary function of *Sirt1* in podocytes is a protection of the cells under the pathological condition rather than the maintenance of the cells in a physiological state.

I have some limitations in this study. The first point is that podocyte-specific deletion of *Sirt1* was not verified completely. However, I utilized Cre-recombinase / loxP system to make podocyte-specific Sirt1 knockout mice, which is widely approved and reported in many previous studies[64–67]. In addition, I confirmed that the expression of SIRT1 was decreased by western blot analysis using isolated glomeruli of experimental mice. Therefore, it is reasonable to regard the podocin-Cre positive and *Sirt1*$^{flox/flox}$ mice I made as podocyte-specific *Sirt1* knockout mice. Secondly, the causal relationship between cytoplasmic cortactin and actin fiber derangement was assessed insufficiently. To specify the interaction between cortactin and actin fiber, actin cytoskeleton derange-

ment by cortactin knock down or inhibition of nuclear export of cortactin should be observed. In addition, immunoprecipitation for investigating the interaction between actin fiber and cortactin may be helpful to demonstrate this problem. Nonetheless, my hypothesis should be acceptable since cortactin is generally considered as an actin fiber-binding protein, even in podocytes, and my data also demonstrated that the dissociation of cortactin from actin fiber by SIRT1 inhibition surely induced actin cytoskeleton derangement. Finally, I could not confirm the total cortactin localization *in vivo* because the antibodies to cortactin we used did not work for IHC. Further investigation is necessary to confirm the localization and distribution of cortactin in the experimental mice.

In conclusion, I found that SIRT1 deacetylates cortactin in the nucleus, and that the deacetylated cortactin in cytoplasm predominantly interacts with actin fibers to enhance maintenance of actin cytoskeleton in podocytes. In contrast, inhibition of SIRT1 enhances the accumulation of acetylated cortactin in the nucleus and accelerates actin cytoskeleton derangement. The SIRT1-cortactin-actin fiber interaction regulates podocyte homeostasis and protects the cells against pathogenic conditions, suggesting that the optimization of SIRT1 activity may be important for podocyte biology.

Acknowledgments

Disclosure

No conflicts of interest are declared.

References

[1]   J. Reiser, V. Gupta, and A. D. Kistler, "Toward the development of podocyte-specific drugs.," *Kidney Int.*, vol. 77, no. 8, pp. 662–8, Apr. 2010.

[2]   V. D. D'Agati, F. J. Kaskel, and R. J. Falk, "Focal segmental glomerulosclerosis.," *N. Engl. J. Med.*, vol. 365, no. 25, pp. 2398–411, Dec. 2011.

[3]   R. C. Wiggins, "The spectrum of podocytopathies: a unifying view of glomerular diseases.," *Kidney Int.*, vol. 71, no. 12, pp. 1205–14, Jun. 2007.

[4]   J. Bariéty, P. Bruneval, A. Meyrier, C. Mandet, G. Hill, and C. Jacquot, "Podocyte involvement in human immune crescentic glomerulonephritis.," *Kidney Int.*, vol. 68, no. 3, pp. 1109–19, Sep. 2005.

[5]   V. Besse-Eschmann, M. Le Hir, N. Endlich, and K. Endlich, "Alteration of podocytes in a murine model of crescentic glomerulonephritis.," *Histochem. Cell Biol.*, vol. 122, no. 2, pp. 139–49, Aug. 2004.

[6]   J.-K. Guo, A. L. Menke, M.-C. Gubler, A. R. Clarke, D. Harrison, A. Hammes, N. D. Hastie, and A. Schedl, "WT1 is a key regulator of podocyte function: reduced expression levels cause crescentic glomerulonephritis and mesangial sclerosis.," *Hum. Mol. Genet.*, vol. 11, no. 6, pp. 651–9, Mar. 2002.

[7]   J. Oh, J. Reiser, and P. Mundel, "Dynamic (re)organization of the podocyte actin cytoskeleton in the nephrotic syndrome.," *Pediatr. Nephrol.*, vol. 19, no. 2, pp. 130–7, Feb. 2004.

[8]   J. Reiser and S. Sever, "Podocyte biology and pathogenesis of kidney disease.," *Annu. Rev. Med.*, vol. 64, pp. 357–66, Jan. 2013.

[9]   L. Guarente, "Sirtuins, Aging, and Medicine," *N. Engl. J. Med.*, vol. 364, no. 23, pp. 2235–2244, 2011.

[10]   J. a Baur, "Biochemical effects of SIRT1 activators.," *Biochim. Biophys. Acta*, vol. 1804, no. 8, pp. 1626–34, Aug. 2010.

[11]   Y. Nakahata, M. Kaluzova, B. Grimaldi, S. Sahar, D. Chen, L. P. Guarente, and P. Sassone-corsi, "The NAD+ -Dependent Deacetylase SIRT1 Modulates CLOCK- Mediated Chromatin Remodeling and Circadian Control," *Cell*, vol. 134, no. 2, pp. 329–340, 2008.

[12] G. Asher, D. Gatfield, M. Stratmann, and H. Reinke, "SIRT1 regulates circadian clock gene expression through PER2 deacetylation," *Cell*, vol. 134, no. 2, pp. 317–328, 2008.

[13] C. Cantó, Z. Gerhart-hines, J. N. Feige, M. Lagouge, J. C. Milne, P. J. Elliott, P. Puigserver, and J. Auwerx, "AMPK regulates energy expenditure by modulating NAD + metabolism and SIRT1 activity," *Nature*, vol. 458, no. 7241, pp. 1056–1060, 2009.

[14] Takashi Nakagawa and Leonard Guarente, "Sirtuins at a glance," *J. Cell Sci.*, vol. 124, no. 6, pp. 833–838, 2011.

[15] F. Yeung, J. Hoberg, and C. Ramsey, "Modulation of NF-κB-dependent transcription and cell survival by the SIRT1 deacetylase," *EMBO J.*, vol. 23, no. 12, pp. 2369–2380, 2004.

[16] M. Lagouge, C. Argmann, and Z. Gerhart-Hines, "Resveratrol improves mitochondrial function and protects against metabolic disease by activating SIRT1 and PGC-1α," *Cell*, vol. 127, no. 6, pp. 1109–1122, 2006.

[17] W. Y. Chen, D. H. Wang, R. C. Yen, J. Luo, W. Gu, and S. B. Baylin, "Tumor suppressor HIC1 directly regulates SIRT1 to modulate p53-dependent DNA-damage responses.," *Cell*, vol. 123, no. 3, pp. 437–48, Nov. 2005.

[18] R. Firestein, G. Blander, and S. Michan, "The SIRT1 deacetylase suppresses intestinal tumorigenesis and colon cancer growth," *PLoS One*, vol. 3, no. 4, p. e2020, 2008.

[19] W. Qin, T. Yang, L. Ho, Z. Zhao, and J. Wang, "Neuronal SIRT1 activation as a novel mechanism underlying the prevention of Alzheimer disease amyloid neuropathology by calorie restriction," *J. Biol. Chem.*, vol. 281, no. 31, pp. 21745–21754, 2006.

[20] R. Wang, Y. Zheng, H. Kim, X. Xu, and L. Cao, "Interplay among BRCA1, SIRT1, and Survivin during BRCA1-associated tumorigenesis," *Mol. Cell*, vol. 32, no. 1, pp. 11–20, 2008.

[21] a. Planavila, R. Iglesias, M. Giralt, and F. Villarroya, "Sirt1 acts in association with PPAR to protect the heart from hypertrophy, metabolic dysregulation, and inflammation," *Cardiovasc. Res.*, vol. 90, no. 2, pp. 276–284, Nov. 2010.

[22] C.-M. Hao and V. H. Haase, "Sirtuins and their relevance to the kidney.," *J. Am. Soc. Nephrol.*, vol. 21, no. 10, pp. 1620–7, Oct. 2010.

[23] M. Kitada, S. Kume, A. Takeda-Watanabe, K. Kanasaki, and D. Koya, "Sirtuins and renal diseases: relationship with aging and diabetic nephropathy.," *Clin. Sci. (Lond).*, vol. 124, no. 3, pp. 153–64, Feb. 2013.

[24] M. Nangaku, Y. Izuhara, N. Usuda, R. Inagi, T. Shibata, S. Sugiyama, K. Kurokawa, C. van Ypersele de Strihou, and T. Miyata, "In a type 2 diabetic nephropathy rat model, the improvement of obesity by a low calorie diet reduces oxidative/carbonyl stress and prevents diabetic nephropathy.," *Nephrol. Dial. Transplant.*, vol. 20, no. 12, pp. 2661–9, Dec. 2005.

[25] I. Mattagajasingh, C.-S. Kim, A. Naqvi, T. Yamamori, T. a Hoffman, S.-B. Jung, J. DeRicco, K. Kasuno, and K. Irani, "SIRT1 promotes endothelium-dependent vascular relaxation by activating endothelial nitric oxide synthase.," *Proc. Natl. Acad. Sci. U. S. A.*, vol. 104, no. 37, pp. 14855–60, Sep. 2007.

[26] J. S. Stern, M. D. Gades, C. M. Wheeldon, and A. T. Borchers, "Calorie Restriction in Obesity : Prevention of Kidney Disease in Rodents," *J. Nutr.*, vol. 131, no. 3, p. 913S–917S, 2001.

[27] P. Pfluger, "Sirt1 protects against high-fat diet-induced metabolic damage," *Proc. Natl. Acad. Sci. U. S. A.*, vol. 1, no. 17, pp. 3–8, 2008.

[28] E. M. Dioum, R. Chen, M. S. Alexander, Q. Zhang, R. T. Hogg, R. D. Gerard, and J. a Garcia, "Regulation of hypoxia-inducible factor 2alpha signaling by the stress-responsive deacetylase sirtuin 1.," *Science (80-.).*, vol. 324, no. 5932, pp. 1289–93, Jun. 2009.

[29] Y. J. Jung, J. E. Lee, A. S. Lee, K. P. Kang, S. Lee, S. K. Park, S. Y. Lee, M. K. Han, D. H. Kim, and W. Kim, "SIRT1 overexpression decreases cisplatin-induced acetylation of NF-κB p65 subunit and cytotoxicity in renal proximal tubule cells.," *Biochem. Biophys. Res. Commun.*, vol. 419, no. 2, pp. 206–10, Mar. 2012.

[30] K. Hasegawa, S. Wakino, K. Yoshioka, S. Tatematsu, Y. Hara, H. Minakuchi, K. Sueyasu, N. Washida, H. Tokuyama, M. Tzukerman, K. Skorecki, K. Hayashi, and H. Itoh, "Kidney-specific overexpression of Sirt1 protects against acute kidney injury by retaining peroxisome function.," *J. Biol. Chem.*, vol. 285, no. 17, pp. 13045–56, Apr. 2010.

[31] S. Kume, T. Uzu, K. Horiike, M. Chin-kanasaki, K. Isshiki, S. Araki, T. Sugimoto, M. Haneda, A. Kashiwagi, and D. Koya, "Calorie restriction enhances cell adaptation to hypoxia through Sirt1-dependent mitochondrial autophagy in mouse aged kidney," *J. Clin. Invest.*, vol. 120, no. 4, pp. 1043–1055, 2010.

[32] W. He, Y. Wang, M. Zhang, and L. You, "Sirt1 activation protects the mouse renal medulla from oxidative injury," *J. Clin. Invest.*, vol. 120, no. 4, pp. 1056–1068, 2010.

[33]   S. Kume, M. Haneda, K. Kanasaki, T. Sugimoto, S. Araki, M. Isono, K. Isshiki, T. Uzu, A. Kashiwagi, and D. Koya, "Silent information regulator 2 (SIRT1) attenuates oxidative stress-induced mesangial cell apoptosis via p53 deacetylation.," *Free Radic. Biol. Med.*, vol. 40, no. 12, pp. 2175–82, Jun. 2006.

[34]   S. Kume, M. Haneda, K. Kanasaki, T. Sugimoto, S. Araki, K. Isshiki, M. Isono, T. Uzu, L. Guarente, A. Kashiwagi, and D. Koya, "SIRT1 inhibits transforming growth factor beta-induced apoptosis in glomerular mesangial cells via Smad7 deacetylation.," *J. Biol. Chem.*, vol. 282, no. 1, pp. 151–8, Jan. 2007.

[35]   P. Y. Chuang, Y. Dai, R. Liu, H. He, M. Kretzler, B. Jim, C. D. Cohen, and J. C. He, "Alteration of forkhead box O (foxo4) acetylation mediates apoptosis of podocytes in diabetes mellitus.," *PLoS One*, vol. 6, no. 8, p. e23566, Jan. 2011.

[36]   Y. Yuan, S. Huang, W. Wang, Y. Wang, P. Zhang, C. Zhu, G. Ding, B. Liu, T. Yang, and A. Zhang, "Activation of peroxisome proliferator-activated receptor-γ coactivator 1α ameliorates mitochondrial dysfunction and protects podocytes from aldosterone-induced injury.," *Kidney Int.*, vol. 82, no. 7, pp. 771–89, Oct. 2012.

[37]   M. J. Moeller, S. K. Sanden, A. Soofi, R. C. Wiggins, and L. B. Holzman, "Podocyte-specific expression of cre recombinase in transgenic mice.," *Genesis*, vol. 35, no. 1, pp. 39–42, Jan. 2003.

[38]   T. Matsusaka, T. Asano, F. Niimura, M. Kinomura, A. Shimizu, A. Shintani, I. Pastan, A. B. Fogo, and I. Ichikawa, "Angiotensin receptor blocker protection against podocyte-induced sclerosis is podocyte angiotensin II type 1 receptor-independent.," *Hypertension*, vol. 55, no. 4, pp. 967–73, Apr. 2010.

[39]   T. Wada, J. W. Pippin, Y. Terada, and S. J. Shankland, "The cyclin-dependent kinase inhibitor p21 is required for TGF-beta1-induced podocyte apoptosis.," *Kidney Int.*, vol. 68, no. 4, pp. 1618–29, Oct. 2005.

[40]   K. C. Kirkbride, B. H. Sung, S. Sinha, and A. M. Weaver, "Cortactin: A multifunctional regulator of cellular invasiveness," *Cell Adh. Migr.*, vol. 5, no. 2, pp. 187–198, Mar. 2011.

[41]   T. D. Pollard and G. G. Borisy, "Cellular motility driven by assembly and disassembly of actin filaments.," *Cell*, vol. 112, no. 4, pp. 453–65, Feb. 2003.

[42]   C. Rigothier, P. Auguste, G. I. Welsh, S. Lepreux, C. Deminière, P. W. Mathieson, M. a Saleem, J. Ripoche, and C. Combe, "IQGAP1 interacts with components of the slit diaphragm

complex in podocytes and is involved in podocyte migration and permeability in vitro.," *PLoS One*, vol. 7, no. 5, p. e37695, Jan. 2012.

[43] P. Mundel and J. Reiser, "Proteinuria: an enzymatic disease of the podocyte?," *Kidney Int.*, vol. 77, no. 7, pp. 571–80, Apr. 2010.

[44] X. Zhang, Z. Yuan, Y. Zhang, S. Yong, A. Salas-Burgos, J. Koomen, N. Olashaw, J. T. Parsons, X.-J. Yang, S. R. Dent, T.-P. Yao, W. S. Lane, and E. Seto, "HDAC6 modulates cell motility by altering the acetylation level of cortactin.," *Mol. Cell*, vol. 27, no. 2, pp. 197–213, Jul. 2007.

[45] D. Kaluza, J. Kroll, S. Gesierich, T.-P. Yao, R. a Boon, E. Hergenreider, M. Tjwa, L. Rössig, E. Seto, H. G. Augustin, A. M. Zeiher, S. Dimmeler, and C. Urbich, "Class IIb HDAC6 regulates endothelial cell migration and angiogenesis by deacetylation of cortactin.," *EMBO J.*, vol. 30, no. 20, pp. 4142–56, Oct. 2011.

[46] Y. Zhang, M. Zhang, H. Dong, S. Yong, X. Li, N. Olashaw, P. a Kruk, J. Q. Cheng, W. Bai, J. Chen, S. V Nicosia, and X. Zhang, "Deacetylation of cortactin by SIRT1 promotes cell migration.," *Oncogene*, vol. 28, no. 3, pp. 445–60, Jan. 2009.

[47] K. Ichimura, H. Kurihara, and T. Sakai, "Actin Filament Organization of Foot Processes in Rat Podocytes," *J. Histochem. Cytochem.*, vol. 51, no. 12, pp. 1589–1600, Dec. 2003.

[48] K. Tryggvason, J. Patrakka, and J. Wartiovaara, "Hereditary proteinuria syndromes and mechanisms of proteinuria.," *N. Engl. J. Med.*, vol. 354, no. 13, pp. 1387–401, Mar. 2006.

[49] C.-K. Chiang and R. Inagi, "Glomerular diseases: genetic causes and future therapeutics.," *Nat. Rev. Nephrol.*, vol. 6, no. 9, pp. 539–54, Sep. 2010.

[50] K. Asanuma, E. Yanagida-Asanuma, C. Faul, Y. Tomino, K. Kim, and P. Mundel, "Synaptopodin orchestrates actin organization and cell motility via regulation of RhoA signalling.," *Nat. Cell Biol.*, vol. 8, no. 5, pp. 485–91, May 2006.

[51] S.-W. Min, P. D. Sohn, S.-H. Cho, R. a Swanson, and L. Gan, "Sirtuins in neurodegenerative diseases: an update on potential mechanisms.," *Front. Aging Neurosci.*, vol. 5, Jan. 2013.

[52] C. Lu and C. B. Thompson, "Metabolic regulation of epigenetics.," *Cell Metab.*, vol. 16, no. 1, pp. 9–17, Jul. 2012.

[53] P. Martínez-Redondo and A. Vaquero, "The diversity of histone versus nonhistone sirtuin substrates.," *Genes Cancer*, vol. 4, no. 3–4, pp. 148–63, Mar. 2013.

[54] S. K. Singh, C. a Williams, K. Klarmann, S. S. Burkett, J. R. Keller, and P. Oberdoerffer, "Sirt1 ablation promotes stress-induced loss of epigenetic and genomic hematopoietic stem and progenitor cell maintenance.," *J. Exp. Med.*, vol. 210, no. 5, pp. 987–1001, May 2013.

[55] H. Wu, a B. Reynolds, S. B. Kanner, R. R. Vines, and J. T. Parsons, "Identification and characterization of a novel cytoskeleton-associated pp60src substrate.," *Mol. Cell. Biol.*, vol. 11, no. 10, pp. 5113–24, Oct. 1991.

[56] Hong Wu and J. Thomas Parsons, "Cortactin, an 80/85-Kilodalton," *J. Cell Biol.*, vol. 120, no. 6, pp. 1417–1426, 1993.

[57] L. Buday and J. Downward, "Roles of cortactin in tumor pathogenesis.," *Biochim. Biophys. Acta*, vol. 1775, no. 2, pp. 263–73, Jun. 2007.

[58] A. M. Weaver, "Cortactin and tumor invasiveness," *Cancer Lett.*, vol. 265, no. 2, pp. 157–166, 2008.

[59] B. L. Rothschild, A. H. Shim, A. G. Ammer, L. C. Kelley, K. B. Irby, J. a Head, L. Chen, M. Varella-Garcia, P. G. Sacks, B. Frederick, D. Raben, and S. a Weed, "Cortactin overexpression regulates actin-related protein 2/3 complex activity, motility, and invasion in carcinomas with chromosome 11q13 amplification.," *Cancer Res.*, vol. 66, no. 16, pp. 8017–25, Aug. 2006.

[60] T. Kobayashi, M. Notoya, T. Shinosaki, and H. Kurihara, "Cortactin interacts with podocalyxin and mediates morphological change of podocytes through its phosphorylation," *Nephron Exp. Nephrol.*, vol. 113, no. 3, pp. e89–96, 2009.

[61] J. Zhao, S. Bruck, S. Cemerski, L. Zhang, B. Butler, A. Dani, J. a Cooper, and A. S. Shaw, "CD2AP links cortactin and capping protein at the cell periphery to facilitate formation of lamellipodia.," *Mol. Cell. Biol.*, vol. 33, no. 1, pp. 38–47, Jan. 2013.

[62] K. Sadoul, J. Wang, B. Diagouraga, and S. Khochbin, "The tale of protein lysine acetylation in the cytoplasm.," *J. Biomed. Biotechnol.*, vol. 2011, Jan. 2011.

[63] F. Lan, J. M. Cacicedo, N. Ruderman, and Y. Ido, "SIRT1 modulation of the acetylation status, cytosolic localization, and activity of LKB1. Possible role in AMP-activated protein kinase activation.," *J. Biol. Chem.*, vol. 283, no. 41, pp. 27628–35, Oct. 2008.

[64] G. I. Welsh, L. J. Hale, V. Eremina, M. Jeansson, Y. Maezawa, R. Lennon, D. a Pons, R. J. Owen, S. C. Satchell, M. J. Miles, C. J. Caunt, C. a McArdle, H. Pavenstädt, J. M. Tavaré, A.

M. Herzenberg, C. R. Kahn, P. W. Mathieson, S. E. Quaggin, M. a Saleem, and R. J. M. Coward, "Insulin signaling to the glomerular podocyte is critical for normal kidney function.," *Cell Metab.*, vol. 12, no. 4, pp. 329–40, Oct. 2010.

[65]   C. El-Aouni, N. Herbach, S. M. Blattner, A. Henger, M. P. Rastaldi, G. Jarad, J. H. Miner, M. J. Moeller, R. St-Arnaud, S. Dedhar, L. B. Holzman, R. Wanke, and M. Kretzler, "Podocyte-specific deletion of integrin-linked kinase results in severe glomerular basement membrane alterations and progressive glomerulosclerosis.," *J. Am. Soc. Nephrol.*, vol. 17, no. 5, pp. 1334–44, May 2006.

[66]   J. Ho, K. H. Ng, S. Rosen, A. Dostal, R. I. Gregory, and J. a Kreidberg, "Podocyte-specific loss of functional microRNAs leads to rapid glomerular and tubular injury.," *J. Am. Soc. Nephrol.*, vol. 19, no. 11, pp. 2069–75, Nov. 2008.

[67]   D. B. Johnstone, O. Ikizler, J. Zhang, and L. B. Holzman, "Background strain and the differential susceptibility of podocyte-specific deletion of Myh9 on murine models of experimental glomerulosclerosis and HIV nephropathy.," *PLoS One*, vol. 8, no. 7, p. e67839, Jan. 2013.